Validity of Equilibrium Beach Profiles

Amin Riazi

Submitted to the
Institute of Graduate Studies and Research
in partial fulfillment of the requirements for the degree of

Doctor of Philosophy
in
Civil Engineering

Eastern Mediterranean University
August 2017
Gazimağusa, North Cyprus

Approval of the Institute of Graduate Studies and Research

Prof. Dr. Mustafa Tümer
Director

I certify that this thesis satisfies the requirements as a thesis for the degree of Doctor of Philosophy in Civil Engineering.

Assoc. Prof. Dr. Serhan Şensoy
Chair, Department of Civil Engineering

We certify that we have read this thesis and that in our opinion it is fully adequate in scope and quality as a thesis for the degree of Doctor of Philosophy in Civil Engineering.

Assoc. Prof. Dr. Umut Türker
Supervisor

Examining Committee

1. Prof. Dr. Şevket Çokgör
2. Prof. Dr. Ahmet Doğan
3. Assoc. Prof. Dr. Umut Türker
4. Asst. Prof. Dr. İbrahim Bay
5. Asst. Prof. Dr. Burhan Yıldız

ABSTRACT

In analytical approaches, beach profiles are estimated based on the assumption that the equilibrium condition is reached. Under this assumption, a variety of models have been proposed in the literature with an attempt to estimate a beach profile with the help of accessible variables like particle settling velocity. The study reported in this thesis was conducted to increase the accuracy of beach profile estimations. In this regard, initially, the particle settling velocity predictions were improved. In the interest of particle settling velocity, a new search splitting pattern through genetic algorithm, has been proposed that can be used to optimize the settling velocity equation with a high degree of accuracy. However, it was realized that the beach profile estimations were not significantly enhanced through the improvements. In particular, it was deemed necessary to investigate whether the difference between an actual and an estimated equilibrium beach profile (EBP) was due to the limitations in the equilibrium beach profile methodology or the identified profile was, in fact, out of equilibrium. Therefore, it was thought imperative to first verity if a profile has reached its equilibrium condition. To this end, in this thesis, a boundary based profile scale factor is proposed, which through a normalized coordinate system, will lead to a unique global profile scale factor. The global profile scale factor is then employed to determine an initial linear beach profile. The amount of erosion and accretion that causes the initial linear profile to transform to the natural EBP is calculated. Accordingly, the balance between the amount of erosion and accretion will identify a turning point distinguishing the erosion and accretion areas on the profile. This turning point helps to evaluate whether the profile is in equilibrium condition or not. The proposed model was validated through various beach profiles resulting in high degrees of accuracy and reliability as presented in the thesis.

Keywords: Cross-shore, Equilibrium beach profile, Morphodynamics, Nearshore, Normalized coordinate system, Profile scale factor.

ÖZ

Birçok analitik yaklaşımda kıyı profilleri denge durumuna ulaşıldığı varsayımına dayanarak tahmin edilmektedir. Bu varsayım altında, partikül çökelme hızı gibi değişkenler yardımıyla kıyı profilini hesaplama girişimi çeşitli farklılıklar gösteren modeller yardımıyla literatürde önerilmiştir. Bu tez çalışması, kıyı profili tahminlerinin denge durumuna ulaşıldığı varsayımının doğruluğunu artırmak için yapılmıştır. Bu bağlamda, başlangıçta, partikül çökelme hızı için farklı araştırmacılar tarafından geliştirilen modeller modifiye edilerek kıyı profili tahminleri iyileştirilmeye çalışıldı. Parçacık çökelme hızı hesaplarının geliştirilmesi ve modifikasyonu için genetik algoritma yoluyla yeni bir arama bölme paterni önerilmiş ve çökelme hızının yüksek derecede doğrulukla optimize edilmesi sağlanmıştır. Sonuçta, çökelme hızında elde edilen iyileştirilmenin kıyı profili tahminlerinin optimize edilmesine önemli ölçüde katkı koymadığı anlaşılmıştır. Bu sonuçlar kıyı denge profili modellerinde özellikle, gerçek ve teorik profil arasındaki büyük farkların metodolojideki sınır şartlarının belirlenmesinden kaynaklandığını veya tanımlanan profilin aslında denge dışı olduğunu araştırmak gerektiğini ortaya çıkarmıştır. Bu amaçla, bu tezde, normalleştirilmiş koordinat sistemi vasıtasıyla özgün bir profil ölçeği yaratacak sınır şartlarının koşullarıyla tanımlanmış profil ölçek faktörü önerilmektedir. Daha sonra, orijinal doğrusal kıyı profilini belirleyerek bu profilin doğal denge profiline dönüşmesine neden olan erozyon ve birikme miktarı hesaplanmıştır. Buna göre, erozyon miktarı ile birikim miktarı arasındaki denge, profil üzerindeki erozyon ve yığılma alanlarını ayıran bir dönüşüm noktası belirlemektedir. Bu dönüşüm noktası, profilin denge durumunda olup olmadığını değerlendirmeye yardımcı olmaktadır. Önerilen model, çeşitli kıyı profilleri vasıtasıyla doğrulanmış ve yüksek derecede

güvenilirlik sağlamıştır.

Anahtar kelimeler: Kıyı çizgisi, Denge kıyı profili, Morfodinamik, Yakın kıyılar, Normalleştirilmiş koordinat sistemi, Profil ölçek faktörü.

Dedicated to those who I care and love the most;

my generous dad, my caring mom,

and my lovely wife:

Mehdi, Mahvash and Mahdieh

ACKNOWLEDGMENT

After an intensive period of nine semesters, today is the day. Writing this note of thanks is the finishing touch on my thesis. First of all, I would like to acknowledge and express my gratitude to my Department, where, I developed amazing practical and academic experiences. Secondly, I would like to thank Assoc. Prof. Dr. Serhan Şensoy, who during a period of high pressure getting prepared for ABET accreditation, I had the pleasure to work with him and learn a lot from his valuable experiences.

I would like to have a special thank you to my amazing supervisor Assoc. Prof. Dr. Umut Türker. Without him this study was impossible. His guidelines were not limited to this thesis. He truly made these nine semesters for me an easy, smooth, and enjoyable journey.

My deepest appreciation belongs to my family. My Mom and dad. All I have and achieved is because of them. With their encouragements, guidelines, and all the supports I needed, I rarely faced with any uncertainty or fear through this challenging journey. My lovely wife, Mahdieh, is the one that made the impossible, possible. During these nine semesters we faced lots of ups and downs, and truly, she was the one holding it all together and making life warm and pleasant.

TABLE OF CONTENTS

LIST OF TABLES

LIST OF FIGURES

LIST OF SYMBOLS

A	Profile Scale Factor ($m^{1/3}$)
A_c	Boundary Based Profile Scale Factor ($m^{1/3}$)
a and b	Empirical Coefficients
a_1	Constant Number
a_2	Wave Decay Constant
b_1, b_2, b_3, b_4, and b_5	Empirical Coefficients
C_D	Particle Drag Coefficient
D	Sediment Particle Size (m)
d_1, d_2, and d_3	Lengths of Longest, Intermediate, and Shortest Axes of the Particle (m)
d*	Dimensionless Diameter
D*(d)	Uniform Energy Dissipation per Unit Volume (Nm/m^3)
F	Wave Energy Flux (J/ms)
g	Gravitational Acceleration (m/s^2)
h	Local Wave Height (m)
h_b	Water Depth at Wave Breaker Location (m)
H_b	Wave Breaker Height (m)
h_i	Water Depth Positive Downwards (m)
k	Breaking Index
M, N and n	Shape Dependent Coefficients

S	Particle Specific Gravity
S_f	Particle Corey Shape Factor
T	Wave Period (s)
X_L	Average Distance Traveled by Sedimentary Particle (m)
y	Seaward Distance (m)
y_i	Horizontal Distance (m)
y^* and h^*	Normalized Values of y_i and h_i (m/m)
y'	Shore-normal Coordinate Directed Onshore (m)
α	Volume of Water per Unit Width (m^3/m)
ϵ	Volume of Erosion per Unit Width (m^3/m)
ρ	Density of Water (kg/m^3)
ω	Particle Settling Velocity (m/s)

Chapter 1

INTRODUCTION

1.1 Background and statement of the problem

A beach profile is defined as the cross-shore morphology of a beach along a coast. In nature, water level, waves, currents, and geological conditions vary a lot and therefore, a stable beach profile may never develop. It is important to express an expression that can be use to describe beach profile shapes mathematically. Hence, the equilibrium beach profile (EBP) concept has been defined as a unique profile morphology that has adjust its final shape under constant wave conditions and grain size (Bruun, 1954; Larson, 1991; Komar, 1998). Experimentally, as the parameters of a wave approaching the shore can be fixed, the equilibrium profile can be reached. However, in reality the equilibrium beach profile may not be achieved. Ideally, the shape of an EBP is found in terms that in an assumed depth-dependent sediment transport equation the transport is equal to zero. Equilibrium profiles have been studied extensively and it is an important part of almost every formulation of currents, wave dynamics, sediment transport, and shoreline response across the surf zone (Bodge, 1992). EBPs are best used for cases where the bathymetry of a beach is unknown or poorly known and also for long-term applications such as beach response to sea level rise (Özkan-Haller and Brundidge, 2007).

At least three approaches (kinematic, dynamic, and empirical) can be used to develop a theory for equilibrium beach profiles (Dean and Dalrymple, 2002). In kinematic ap-

proach the beach profile is estimated through the motions of an individual sand particle. The specified sand particle can be either suspended or bedload. In dynamic approach, it is accepted that the equilibrium profile occurs when the constructive and destructive forces acting on the bottom of the beach are balanced. In empirical approach, the beach profiles found in nature are analyzed and the equilibrium profile is described based on the most characteristic forms. Generally, in an empirical approach, the average profile over a period of time is referred to the equilibrium beach profile.

Through the mentioned approaches and with the aim of estimating the equilibrium beach profile a variety of empirical and semi-empirical equations have been proposed in the literature. In the process of developing a new approach to estimate the EBP, generally, it is assumed that the employed profiles that will be used to verify the approach are in equilibrium condition. Hence, it should be defined that the difference between an actual and an estimated equilibrium beach profile is due to the limitations in the methodology of the approach, or simply the identified profile has not reached the equilibrium condition.

1.2 Aims and objectives of the research

The main aim of this study is to propose a practical use for Deans (1977) analytical approach that can be employed to improve the models that are used to estimate EBPs. Deans (1977) approach is based on profile shape factor that is a function of particle settling velocity. Hence, as a first try, a novel approach in estimating the particles settling velocity was developed. To improve the accuracy of the new settling velocity equation, it was considered as an optimization problem, and it was optimized through the published dataset in the literature and new experiments conducted in Civil Engineering hydraulic laboratory of Eastern Mediterranean University (EMU). In the optimization process it was recognized that an improved optimization model is required

for engineering problems. Therefore, genetic algorithm was comprehensively studied and a new optimization algorithm was proposed for engineering problems with an emphasize on hydraulic and coastal engineering problems. Subsequently, the new optimized and most accurate settling velocity was used to increase the accuracy of Deans (1977) estimations. However, it was observed that in some cases the estimations were improved where in other cases there was no significant changes. The model was able to estimate some EBPs with a high and some with very low degree of accuracy. The question raised here was that what is the main difference among these profiles? It was obvious that if a profile is out of equilibrium condition an EBP model may not be able to estimate the profile with a high degree of accuracy. Hence, as having an average of couple of profiles over a specified period of time cannot be verified as the EBP and using the average profile instead of EBP can decrease the accuracy of the estimations. In this regard, it is necessary to first verify if a profile is in equilibrium condition. Therefore, this study aims to propose a model where it can be used to verify if the equilibrium condition of a beach profile has been reached or not?

1.3 Research questions

- Why some beach profiles can be estimated with a high degree of accuracy and some are unpredictable?
- In the interest of beach profiles, does improving the particle settling velocity estimations improve the current models in the literature that are based on particle setting velocity?
- Can the new optimization methods like search splitting pattern improve the accuracy of beach profile estimations?
- Is a specified profile in equilibrium condition?

- Is the low accuracy of a model in predicting the equilibrium beach profile because of the profile is out of equilibrium condition?
- Is there any turning point on a profile that the erosion section can be differed from the accretion section?

1.4 The proposed methodology

In the dynamic zone of shoreline up to depth of closure the beach morphodynamics changes constantly. Thus far, as it is illustrated in Figure 1.1, in the approaches presented in the literature, first, the beach profiles are plotted continuously over time. Then by taking the average among the plotted profiles the equilibrium beach profile is estimated. The obtained beach profile is used to develop new approach in estimating the EBP. However, in this process it has not been verified that if the obtained profile is in equilibrium condition and thus it is just an assumption. Herein, a new approach is presented that can be used to verify if profile is in equilibrium condition or not. In this regard, through the depth of closure, a boundary based profile shape factor, *A*, is proposed. In a normalized coordinate system, the proposed *A* will lead to a unique global EBP. With the help of the global EBP the amount of erosion and accretion affecting a profile can be calculated. The balance between the amount of erosion and accretion is employed to decide if a profile is in equilibrium condition or not.

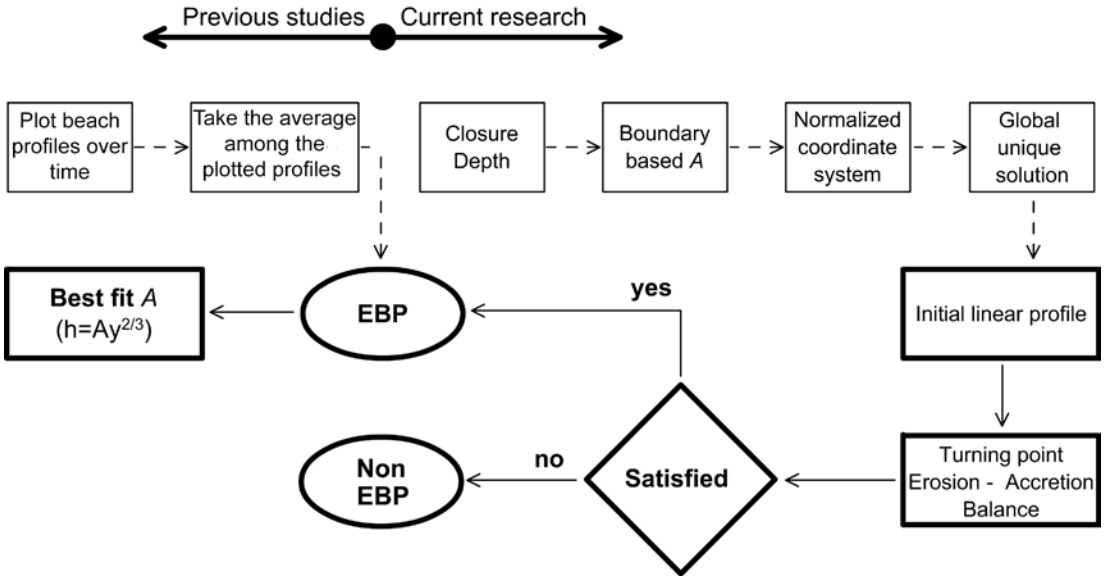

Figure 1.1: Methodology Flow Chart

1.5 Outline of the study

This study consists of six chapters. The first chapter is the introduction where the objectives of the study, information about the contribution of the research to the literature, and target methodology are presented. In the second chapter, the Coastal zone and beach profiles are discussed. In Chapter three the equilibrium beach profiles will be comprehensively reviewed. Chapter four will cover the methodology of this study. In chapter five the results and discussions are presented. The final chapter, chapter six, contains the conclusions and recommendation for further studies.

1.6 Importance of the study

A correct equilibrium beach profile description is essential in quantifying nearshore processes and coastal developments such as the evolution and stability of beaches. The beach profile is the result of the interchange between onshore and offshore fluxes. The direction of the cross-shore fluxes is closely related to the nonlinear characteristics of the incoming waves and it is a key parameter for tools that is used to predict nearshore

processes such as EBPs (da Silva et al., 2006). The concept of equilibrium beach profile is very important in coastal engineering studies. As the process of obtaining the EBP is very complex, it is difficult to simulate it with numerical models and therefore a physical model has been an interesting alternative. The advantage of a physical model is that with constant wave condition an EBP can be reached. The validation of EBP can increase the reliability of the models, reduce the time and cost of a project, and improve the estimations that can lead to consistent project.

1.7 Limitations of the study

This study is based on well-known and widely accepted Dean (1977) theory. Although Deans (1977) approach, due to its analytical background and simplicity, among the complicated and cumbersome approaches it is highly accurate and reliable, it has its own limitations that are inherited. The proposed approach is limited to wave dominated beaches and does not cover the longshore sediment transport and only covers the distance between the shoreline and depth of closure. Moreover, the profile deepens monotonically in the offshore direction with the assumption of uniform particle size distribution.

Chapter 2

COASTAL ZONE AND BEACH PROFILE

2.1 Coastal zone

A majority of the world's population inhabit in coastal zones. The term coastal zone is referred to an extremely dynamic region between the interfaces of the three major natural systems: earth’s surface atmosphere, land surface, and ocean. Although, coastal zones share many similar ecological and economic characteristics, they differ in many geological and biological features. A coastal zone as it is shown in Figure 2.1, can be divided into four main parts: coast, shore or beach, nearshore, and offshore.

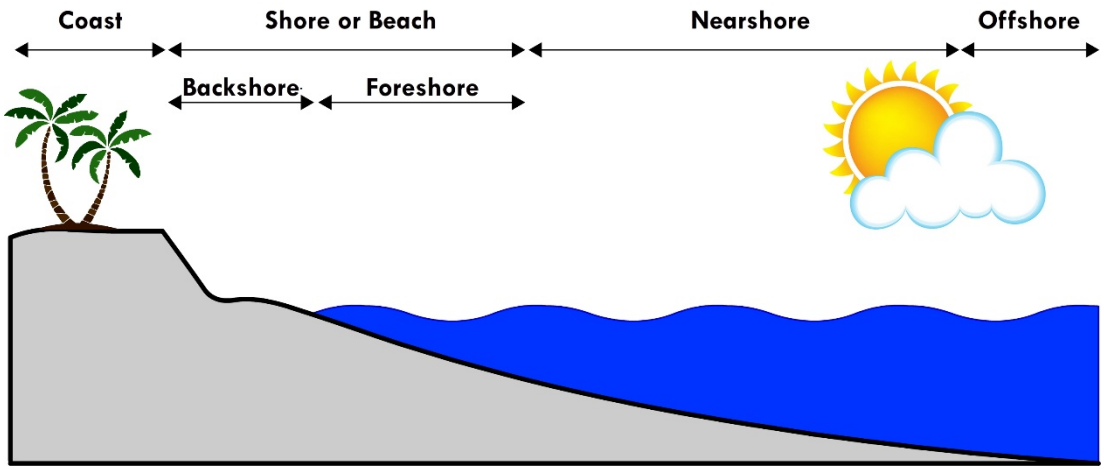

Figure 2.1: Sketch and visual definition of the coastal zone

In general, the area in between a land and ocean is defined as coastal environment. The coastal environment includes both the zone of shallow water and the area landward (beaches, cliffs, and coastal dunes). The shore or beach is subjected to wave action and the shallow water is defined as were the waves are able to move sediment. In terms of

storms, the shore or beach, itself, can be divided into two sections, backshore and foreshore portion, where backshore section is subjected to wave action only during storms and foreshore section is subjected to wave action during non-storm conditions (Davidson-Arnott, 2010). Nearshore zone starts after the beach and the seaward limit is where the offshore is defined. In nearshore region significant sediment transport is done by waves (Masselink et al., 2014). The offshore boundary is generally defined as the water depth where the orbital motion associated with the largest storm waves is no longer able to affect the bed significantly or to transport sediment. The mentioned offshore point, were the depth changes over time are negligible is denoted the depth of closure (Hartman and Kennedy, 2016).

2.2 Beaches

Beach morphology is affected by wave climates, tide range, and sediment characteristics. Roughly, beaches can be classified into three groups of wave dominated, tide modified, and tide dominated beaches. Wave dominated beaches are those subjected to low tides and the sediment transport is due to wave action. Tide dominated beaches form in areas of high tide range. In tide dominated beaches tides are the cause of significant sediment transport and predominates over the effects of waves (Heward, 1981). Tide modified beaches can be defined as beaches in between the wave and tide dominated beaches.

Current study is on wave dominated beaches. On wave dominated beaches the swash zone connects the dry beach with the surf and it is the steeper part of the shoreline across which the broken waves run up and down across the beach face. Based on wave and sand properties, wave-dominated beaches can be divided into three main types: reflective, intermediate, and dissipative (McArdle and McLachlan, 1992). As it is

shown in Fig. 2.2, dissipative beaches due to high waves and fine sands have a wide surf zones usually with two or three shore-parallel bars. Intermediate beaches which are intermediate between the lower energy reflective beaches and the highest energy dissipative beaches, contain fine to medium sands. The most obvious characteristic of intermediate beaches is the presence of a surf zone with bars and rips. Lower waves will cause reflective beaches with coarser sand.

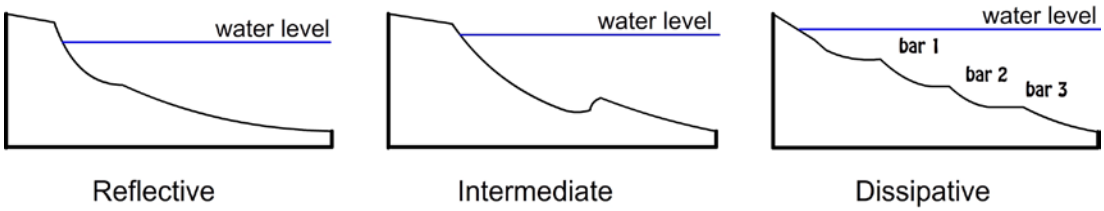

Figure 2.2: Conceptual beach models: Reflective, Intermediate, and Dissipative (Adopted from Masselink and Short, 1993)

Reflective beaches always have a steep, narrow beach and swash zone. In reflective beaches as waves move unbroken to the shore and collapse or surge up the beach face, bars and surf zone are absent (Short, 2005). If there is a mixture of sediment size, then the coarsest material accumulates at the base of the swash zone (at around low tide level) and forms a coarse steep step, up to several decimeters high. Immediately seaward of the step is a low gradient near shore (wave shoaling) zone composed of finer sediment.

2.2.1 Beach profiles

The shape of any surface is called its morphology; hence beach morphology refers to the shape of the beach, surf and nearshore zone. As all beaches are composed of sediment deposited by waves, beach morphology reflects the interaction between waves of a certain height, length and direction and the available sediment; whether it be sand, cobbles or boulders; together with any other structures such as headlands, reefs and

inlets (Short, 2000). A beach profile, Figure 2.3, represents the cross-shore morphology of the beach along the coast (Kaiser & Frihy, 2009).

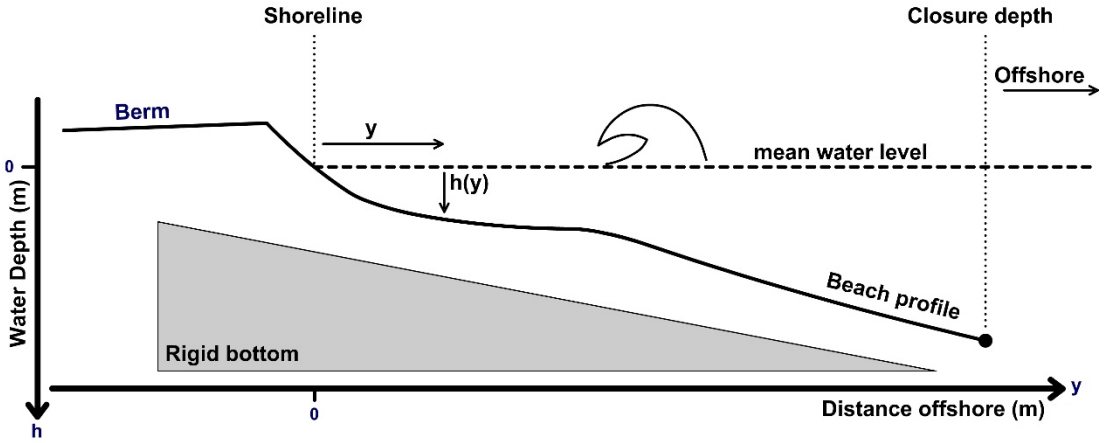

Figure 2.3: A sketch of beach profile. The still-water depth is defined as a function of horizontal distance from the shoreline *h(y)*.

A beach profile is shaped by the natural forces affecting the sand making up the beach (Dean & Dalrymple, 2004). The size of beach sand determines its contribution to beach dynamics. Sediments fall through water at a speed which is proportional to its size (Short, 2000). The fall velocity of the sediments directly affects the profile shape. The profile shape in between the shoreline up to depth of closure is highly dynamic and changes constantly. Having an approach that can consider all the variables effecting the beach profile and be able to estimate accurate beach profiles is yet impossible. Hence, the dynamic behavior of beach profile makes the concept of equilibrium beach profile important.

2.2.2 Equilibrium beach profile

For a beach with specific sand size and engaged to a constant breaking waves, the equilibrium beach profile is defined as a shape that has no net change in time (Larson, 1991). There are different approaches in estimating EBPs. Theoretically and based on dynamic approach, the result of the balance between the destructive and constructive forces is considered as the equilibrium beach profile. In an empirical approach, beach

profiles are plotted over a wide range of time period and the graphical average of all the plotted profiles is considered as the representative EBP. In the kinematic approach, the motions of an individual sand particle is considered. This approach seems to be highly accurate and complete. However, considering how many particles are in a beach profile, this approach is beyond our present state of knowledge. The concept of an equilibrium beach profile has become a guiding principle behind the development of most shoreline change models (Pilkey et al., 1993; Are & Reimnitz, 2008) and it has been a part of the ideas in use in coastal engineering studies. At a specific coastal zone, the steepness and morphological features of a predicted EBP is mainly based on the grain size characteristics of the beach. In many field studies, it has been recognized that coarser beaches are characterized by steeper slopes. In contrast, finer beaches show gentle slope profiles (Kaiser & Frihy, 2009). To verify if a profile is in equilibrium condition requires extensive field measurement of beach profiles (Pilkey et al., 1993).

Chapter 3

EQUILIBRIUM BEACH PROFILES

3.1 Introduction

There are different destructive and constructive forces affecting beach profiles. If a beach with a specific sediment size is exposed to a constant force condition, although sediments will be in motion, it will develop a profile shape that displays no net change in time. In numerical simulation and based on a given wave height and water level condition, it is assumed that a beach profile will always end up with its most stable or equilibrium form (Titus, 1985). Since 1950s the beach equilibrium condition and profile shapes have been studied. Equilibrium profile models have been widely used for predicting beach changes in the cross-shore direction. The validity and significance of the equilibrium beach profile equation can be evaluated through extensive field measurements. This has encouraged many researchers to develop mathematical relationships to define the profile shape. In this section, previous studies will be reviewed.

3.2 Theoretical EBPs expressions

The most common beach profile expression is extracted by Bruun (1954) and Dean (1977).

$$h(y) = A(d)y^{\frac{2}{3}} \tag{3.1}$$

where h is the water depth at a seaward distance y, A is a dimensional parameter that depends primarily on sediment characteristics such as settling velocity and diameter. In the power law Eq. (3.1), Bruun (1954) had assumed that the bottom shear stress and wave energy dissipation were constant at equilibrium. In the interest of a theoretical

approach, for a uniform sediment distributed beach profile, Dean (1977) derived this power law by assuming a constant wave energy dissipation per unit water volume along the profile. Later, Moore (1982) exposed that the constant wave energy dissipation per unit water volume is a function of sediment size.

Moore (1982) was the first researcher who investigated various profiles. As it is shown in Fig. 3.1, he obtained the profile scale factor as a function of effective diameter of the sediments across the surf zone.

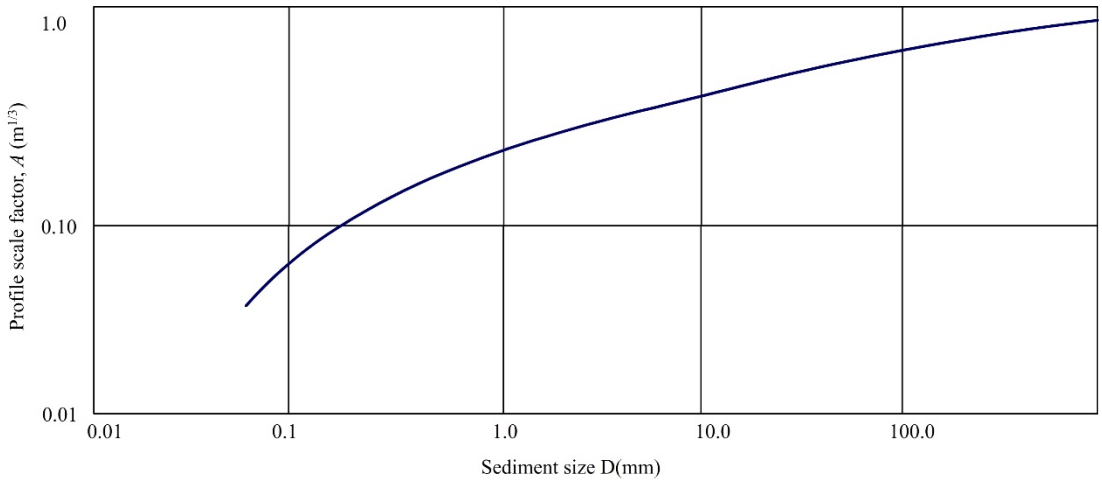

Figure 3.1: Dependence of *A* on sediment grain size (Moore, 1982).

Dean (1987) simply transformed Moore's (1982) relationship and found the simple relationship between the profile scale factor, *A*, and the particle settling velocity ω (cm/s).

$$A = 0.067\omega^{0.44} \qquad (3.2)$$

Later, Boon and Green (1988) did a study on ten carbonate beaches in the Sint Maarten Island located in the extreme northeast corner of the Caribbean Sea at the top of the Lesser Antillean arc system. They connected the values of *A* and *m* to each other through the following equation:

$$A = \left(\frac{0.13}{\left(\frac{H_b^2}{gDT^2} \right)} + 0.12 \right)^m \tag{3.3}$$

where D is the sediment particle size, T is wave period, H_b is wave breaker height and g is acceleration due to gravity.

In the interest of particle settling velocity, Kriebel et al. (1991) by considering a fraction of the wave energy dissipation per unit volume due to wave breaking equal to the energy dissipation associated with suspended sand settling under their own submerged weight, proposed the A in terms of particle settling velocity ω (m/s).

$$A = 2.25 \left(\frac{\omega^2}{g} \right)^{\frac{1}{3}} \tag{3.4}$$

where the settling velocity should be between 0.01 and 0.1 m/s.

Later, Dubois (1999) mentioned that A and m are inversely related to each in the form of an exponential function:

$$A = ae^{-bm} \tag{3.5}$$

where a and b are empirical coefficients that vary from one shore region to another. They have mentioned that, normally, the value of a is within the interval of [3, 17] and the value of b is within the interval of [-7, -4].

Türker and Kabdaşlı (2006) by modifying the wave energy dissipation rate proposed a new definition for profile scale factor:

$$A = \frac{a_1}{(k^2 X_L)^{\frac{2}{3}}} \left[\frac{3}{5} H_b^2 h_b^{-1/2} + a_2^2 h_b^{3/2} \right]^{\frac{2}{3}} \tag{3.6}$$

where a_1 is a constant number equal to 3.285, k is the ratio between wave height and water depth at break, X_L is the average distance traveled by sedimentary particle, a_2 is the wave decay constant (that is equal to 0.4), and h_b is water depth.

In a different approach, Bodge (1992) and Komar and McDougal (1994), proposed the beach profile shape in forms of an exponential function:

$$h(y) = -b_1(1 - e^{-b_2 y}) \tag{3.7}$$

where the two coefficients b_1 and b_2 are estimated by fitting $h(y)$ with field observations. The coefficient b_1 appears to be expressible in terms of aspects of the local incident wave and bottom sediment characteristics. The coefficient b_2 was also correlated with sediment characteristics of the beach. Based on Bodge (1992) field observations b_2 can be considered within the range of $3x10^{-5}$ to $1.16x10^{-3}$ m^{-1} and the coefficient b_1 is within the range of 2.7 to 70 m.

Later, Dai et al. (2007) investigated equilibrium beach profile in South China and proposed a relationship that they argue it can be applied to sectors both above and below the sea-water level.

$$h(y) = b_3 e^{b_4 y} + b_5 \tag{3.8}$$

where the coefficients b_3, b_4, and b_5 are empirical parameters.

3.2.1 EBP: Analytical solution

Among the different approaches discussed in section 3.2, Dean's (1977) approach provides an analytical relationship between profile changes and beach sediment characteristics. The model was developed based on linear wave theory, where the wave energy per unit surface area is considered as:

$$E = \frac{1}{8}\rho g H^2 \tag{3.9}$$

where, ρ is the density of water. The Energy flux, F, group velocity in shallow water, C_g, and spilling break assumption where considered as Eqs. (3.10), (3.11), and (3.12) respectively.

$$F = EC_g \tag{3.10}$$

$$C_g = \sqrt{gh} \tag{3.11}$$

$$H = kh \tag{3.12}$$

where g is the gravity acceleration, H is the local wave height, h is the local water depth, and k is the breaking index which is about 0.78 (CERC, 1984).

Based on the Energy flux and by considering the offshore direction positive, for a given sediment size in terms of the energy conservation, the uniform energy dissipation per unit volume, $D_*(d)$, can be written as:

$$-D_*(d) = \frac{1}{h}\frac{dF}{d\acute{y}} \tag{3.13}$$

where $\acute{y}$ is the shore-normal coordinate directed onshore. Eq. (3.13) states that when the sediment is stable, the average wave energy dissipation per unit volume is equal to the changes in wave energy flux, F, over a certain distance divided by the water depth. To simplify Eq. (3.13) it can be assumed that the wave energy dissipation per unit volume for an equilibrium beach profile is only a function of sediment dimeter, d.

$$-hD_*(d) = \frac{d\left(\frac{1}{8}\rho g k^2 h^2 \sqrt{gh}\right)}{d\acute{y}} \tag{3.14}$$

Taking the derivative and simplifying, the dissipation per unit volume is solved to be:

$$D_*(d) = \frac{5}{16}\rho g^{\frac{3}{2}} k^2 h^{\frac{1}{2}} \frac{dh}{dy} \tag{3.15}$$

Eq. (3.15) illustrates that the dissipation per unit volume has a direct relationship with the square root of the water depth and the beach slope. Moreover, in this equation the onshore coordinate $\acute{y}$ has been changed to offshore direction y, leading to the elimination of the minus sign. In Eq. (3.15) the depth h is the only variable that varies with y, thus we can integrate for h:

$$h(y) = \left(\frac{24D_*(d)}{5\rho g k^2\sqrt{g}}\right)^{\frac{2}{3}} y^{\frac{2}{3}} = A(d)y^{\frac{2}{3}} \qquad (3.16)$$

As mentioned before *y* is oriented in an offshore direction with the origin at the mean water line. The *A* in Eq. (3.16) is a dimensional parameter and it is referred to as the profile scale factor. The profile scale factor is a function of energy dissipation and it is affected indirectly by the sediment size of the beach.

3.3 Literature review

Generally, in most of the models developed for simulating shoreline changes (Hanson and Kraus, 1989), equilibrium beach profile is the main concept. Empirically, it has been tried to validate EBPs. Kaiser and Frihy (2009) have analyzed the main Nile headlands: Abu-Quir bay, Rosetta promontory and Burullus. The measured profiles were compared with the exponential beach profile concept, Eq. (3.7). The results showed that the profiles cannot be described only by an exponential hypothesis. It has been concluded that the beach profiles along the Nile Delta can be described through equilibrium expression. However, one equilibrium profile equation is not sufficient to assess all beach profiles.

Choi et al. (2016) performed laboratory experiments based on wave data measured at the Haeundae coast during 3 years. The experiments were done with two dominant waves: a storm wave and a normal wave. They have conducted that the storm and normal waves did alternately changed the beach profile up to a quasi-equilibrium beach profile that reasonably agreed to the beach profile of the Haeundae beach.

The morphology of beach profiles is required to solve many coastal engineering problems. Hence, different researchers have tried to improve the current equations for different uses. For instance, Aragonés et al. (2016) have developed a new methodology to increase the accuracy of the existing equilibrium beach profile models for Valencia's

beaches. They have conducted that from models obtained by analysis and testing through potential, exponential and logarithmic functions, the potential function provides the best results.

Ludka et al. (2015) tried to give field evidence of beach profile evolution toward equilibrium. They studied profiles from five beaches (medium grain size sand) in southern California. Elevations were observed quarterly for 3 to 10 years. They have conducted that physics-based process models are needed to quantify the complex fluid and sediment dynamics underlying the observed macroscopic equilibrium behavior, to determine the role of the neglected alongshore transport, and to explore causes of model failures.

3.4 Improvement of particle settling velocity

There are a variety of particle settling velocity equations in the literature. Cheng (1997) developed a simplified equation based on a relationship between the particle Reynolds number and particle drag coefficient:

$$\frac{\omega d}{\upsilon} = \left(\sqrt{25 + 1.2d_*^2} - 5\right)^{1.5} \tag{3.17}$$

where ω is particle settling velocity, υ is ambient fluid kinematic viscosity, and d_* , the dimensionless diameter, that is defined as:

$$d_* = d\left(\frac{(S-1)g}{\upsilon^2}\right)^{\frac{1}{3}} \tag{3.18}$$

where *S* is the particle specific gravity, and *g* is gravitational acceleration.

In a similar approach and in order to increase the accuracy of the particle settling velocity estimations, Wu and Wang (2006) proposed an equation based on particle shape:

$$\omega = \frac{M\upsilon}{Nd}\left[\sqrt{0.25 + \left(\frac{4N}{3M^2}d_*^3\right)^{\frac{1}{n}}} - 0.5\right]^n \tag{3.19}$$

where *M*, *N* and *n* are shape dependent coefficients and are defined as:

$$M = 53.5e^{-0.65Sf}$$

$$N = 5.65e^{-2.5Sf} \tag{3.20}$$

$$n = 0.7 + 0.9S_f$$

where S_f is particle Corey shape factor and it is defined as:

$$S_f = \frac{d_3}{\sqrt{d_1 d_2}} \tag{3.21}$$

where d_1, d_2, and d_3 are the lengths of longest, intermediate, and shortest axes of the particle, respectively.

In this study, a different methodology is used to improve the particle settling velocity estimations. In this regard, the particle drag coefficient is considered as a function of particle nominal diameter, gravitational acceleration, the ambient fluid kinematic viscosity, and particle shape defined as Corey shape factor. And the effect of particle specific gravity is only considered in particle settling velocity.

$$\omega^2 = \frac{4}{3}\frac{(S-1)g}{C_D} S_f^{\frac{2}{3}} d_n \tag{3.22}$$

Hence, the particle drag coefficient independent of particle specific gravity is defined as:

$$C_D = \left(\frac{a_4 \times \nu}{d_n^{1.5} \times g^{0.5}} + a_5\right)^{a_2} \tag{3.23}$$

where:

$$a_2 = 2.023$$

$$a_4 = 96.45 - 74.74S_f^{-0.113} \tag{3.24}$$

$$a_5 = 1.129 - 0.435S_f^{1.7}$$

The experimental work of the study was conducted in the hydraulic laboratory of Eastern Mediterranean University. The aim was to capture the motion of sedimentation and

to calculate the settling velocity in order to improve the accuracy of settling velocity estimations. To calculate the nominal diameter and shape factor the three orthogonal diameters of each particle was measured through 3 dimensional photography. The settling process was done in a 2000 mm long and 250 mm diameter clear acrylic tube containing fresh water. The particles were released slightly below the water surface and allowed to fall for 1000 mm to achieve the terminal velocity. Then the settling motion was captured in the following 891 mm by the help of Sony NEX-VG900 digital camcorder. A rechargeable temperature data logger (OMEGA: OM-EL-USB-1-RCG) with resolution of 0.1^{o}C was placed in the middle of the tube and the temperature of the ambient fluid was recorded per second. Different temperatures were used to obtain different ambient fluid kinematic viscosities. The experiments were done in five different temperatures (13.7^{o}C, 14.3 ^{o}C, 27.4 ^{o}C, 27.5 ^{o}C, 28.5 ^{o}C). The experiment durations were limited to 10 minutes in order to avoid temperature variation. All the videos were decoded to frames as a sequence of images to show the motion of the particles settling in the tube in a single image. As it is shown in Fig. 3.2, during the settlement process, particles had different wandering behavior with an apparent different wavelengths and amplitudes. It was observed that particles settle with their largest projected area normal to the settling direction. Similar observations is reported in the literature as well (Smith and Cheung, 2003; Komar and Reimers, 1978).

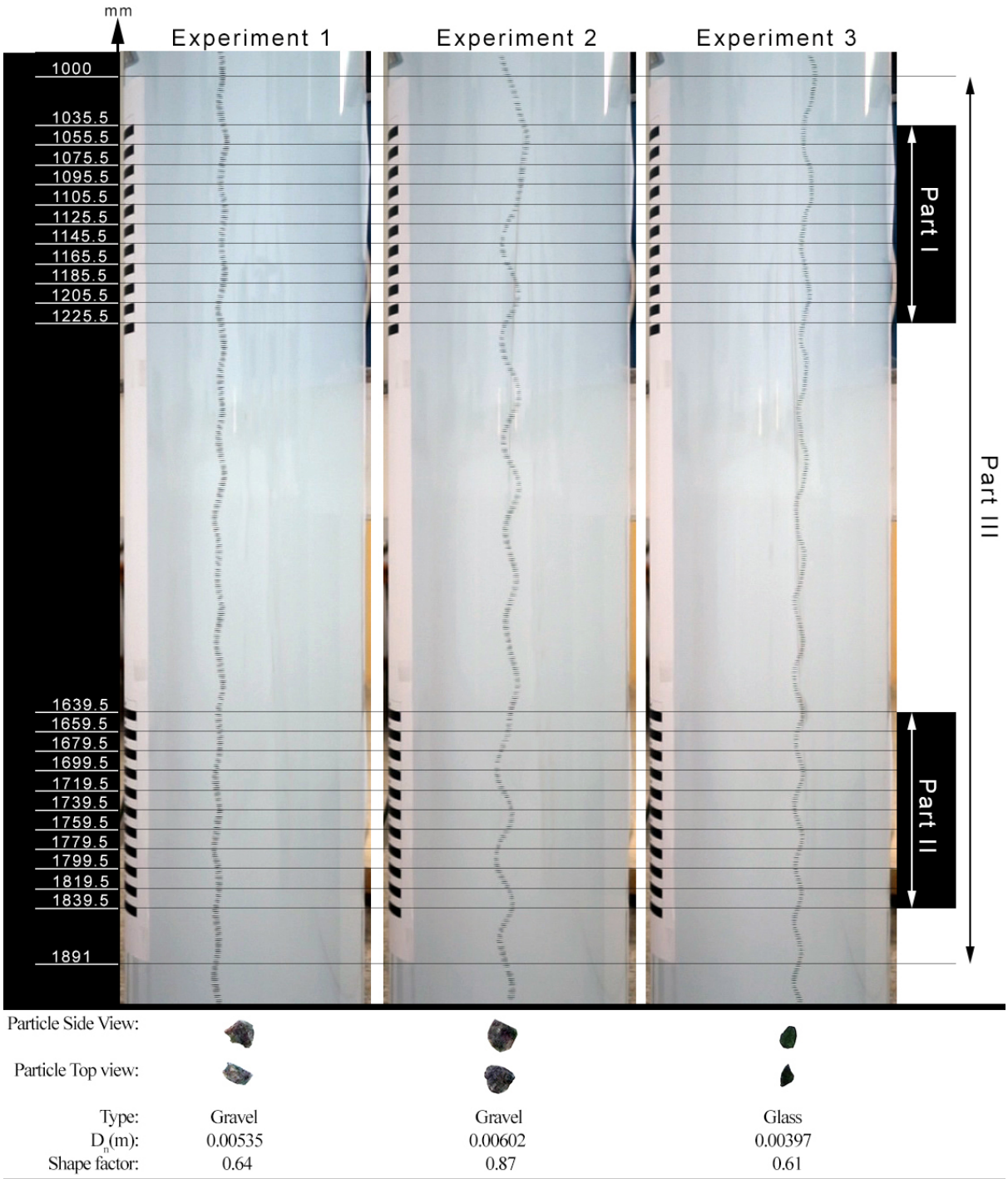

Figure 3.2: Videos converted to a sequence of images. The distance from the base point is given in mm on the left. The velocity measurements were conducted in three parts: Part I, Part II, and Part III.

During each experiment the time necessary for particles to travel through part I and part II in Fig. 3.2 were recorded and compared to make sure that in the main measurement interval (part III) the settling velocity was achieved. Among all the experiments, the 46 particles settling with zero acceleration are listed in Appendix A. The specific

gravity of the particles were measured through pycnometer test.

3.4.1 Results and discussion

The proposed drag coefficient, Eq. (3.23), was compared with drag coefficients proposed by Julien (1995), Cheng (1997), She et al. (2005), Wu and Wang (2006), and Camenen (2007) through MRE. As it is shown in Fig. 3.3, for particle Reynolds number greater than 30, the drag coefficients proposed in the literature estimate higher values in comparison with Eq. (3.23). The overestimations of the drag coefficient in the literature is due to the assumption of spherical particles which is an overestimated value for natural sediment particles. The drag coefficient values obtained by equations proposed by Julien (1995) and She et al. (2005) have considerable deviation from Eq. (3.23). The main reason of this deviation can be attributed to the size and the shape of the particles used in previous studies. As shown in Fig. 3.3, under the condition of high Reynolds numbers (Re>1000) the drag coefficients proposed by Julien (1995) and She et al. (2005) equals to 1.5. However, according to Cheng (1997), for high particle Reynolds number, the drag coefficient of natural sediment particles (S_f = 0.7) should be within the interval of [1.0, 1.2].

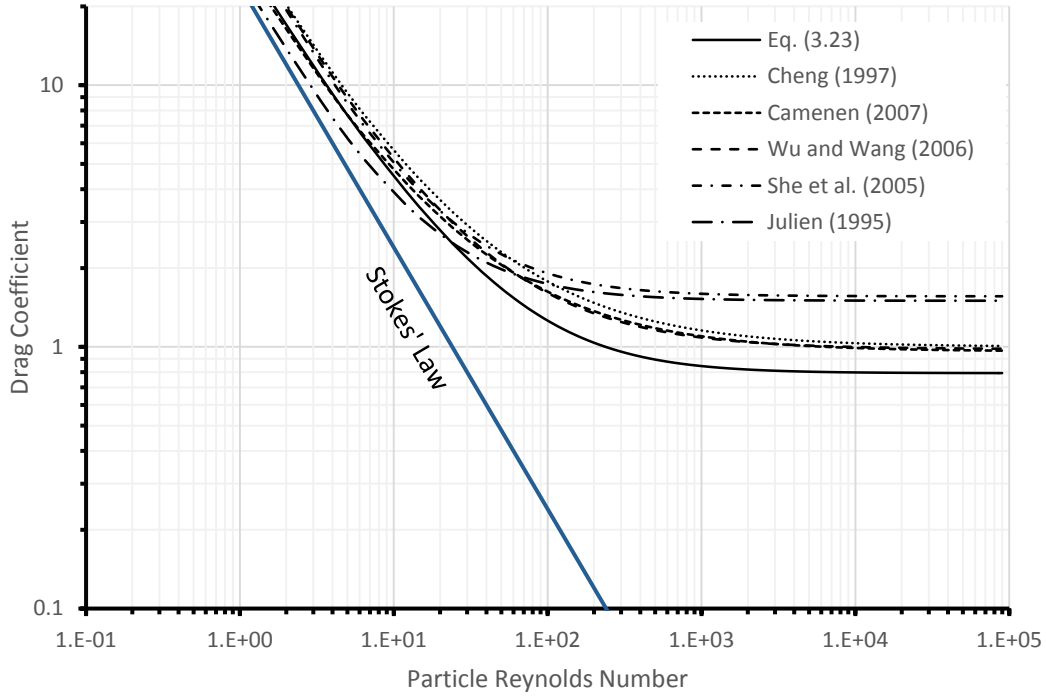

Figure 3.3: The relationship between different drag coefficients and particle Reynolds number for particles with shape factor equal to 0.7

The improvement of drag coefficient increase the accuracy of the settling velocity calculations. In this regard, Eq. (3.22), the settling velocity based on the new drag coefficient defined in this study, is compared with three well-known accurate settling velocity equations proposed by Swamee and Ojha (1991), Wu and Wang (2006), and Camenen (2007). The comparison is done through mean relative error. As the proposed settling velocity equation covers the effect of particle shape factor, in order to illustrate the performance of the equation, the employed dataset was divided into five different groups based on the particles shape factor. As Table 3.1 illustrates the proposed equation shows better performance than the mentioned equations in the complete range of particle shape factor.

Table 3.1: Comparison of different settling velocity equations against data with shape factors through MRE.

Shape factor range	Data Number	Swamee and Ojha (1991)	Wu and Wang (2006)	Camenen (2007)*	Eq. (3.22)
		Mean relative errors (%)			
$0 < S_f \leq 0.2$	4	11.2%	8.1%	36%	4.7%
$0.2 < S_f \leq 0.4$	45	10.5%	6.2%	21%	6.1%
$0.4 < S_f \leq 0.6$	105	12.1%	6.8%	6.8%	6.7%
$0.6 < S_f \leq 0.8$	186	29.4%	6.4%	9.2%	6.3%
$0.8 < S_f \leq 1$	58	21.5%	5.5%	21%	4.4%
Total	398	21.4%	6.3%	11.8%	6.1%

* Roundness factor was selected 3.5 as it was mentioned by Camenen (2007) for Natural sands. For the employed dataset, different roundness numbers were tested and the departure of roundness factor from 3.5 decreases the accuracy of the settling velocity calculated by the equation proposed by Camenen (2007).

The high accuracy of Wu and Wang (2006) equation describes their logical approach to settling velocity. As it can be observed from Table 3.1, the highest accuracy of Wu and Wang (2006) equation is obtained for particles with shape factor within the interval of (0.8, 1]. This high accuracy is in line with the argument that their approach is based on the assumption of spherical particles. The results obtained through Eq. (3.22) shows that the presented approach has improved the accuracy of the settling velocity on the entire range of particle shape factor.

3.5 Effect of particle settling velocity on profile scale factor

Herein, the effect of three different particle settling velocity equations, mentioned in section 3.4, on profile scale factor is investigated.

In Dean's (1977) analytical approach, the profile scale factor, *A*, has not been directly defined. Hence, researches have tried to obtain the value of *A* through accessible parameters. Therefore, as it was mentioned earlier, Eqs. (3.2) and (3.4) have defined *A* in terms of particle settling velocity. Hence, improving the particle settling velocity can affect the accuracy of beach profile estimations. It seems necessary to verify the effect of particle settling velocity on profile scale factor.

As illustrated in Table 3.2 the profile scale factor for a specific particle with diameter of 0.05cm has been calculated through different approaches presented above.

Table 3.2: Effect of particle settling velocity on profile scale factor, where the particle diameter is fixed to 0.05 cm, kinematic viscosity has been considered as 0.000001 m^2/s and Corey shape factor to be equal to 0.7.

Approach	Eq. (3.2)	Eq. (3.4)	Difference
Cheng (1997)	0.1481	0.1804	0.032
Wu and Wang (2006)	0.1528	0.1890	0.036
Riazi and Türker (2017c)	0.1520	0.1876	0.036
Average	0.1510	0.1857	0.0347

Based on the obtained values for *A* through different settling velocity equations, equilibrium beach profiles based on Eq. (3.1) are plotted (Fig 3.4).

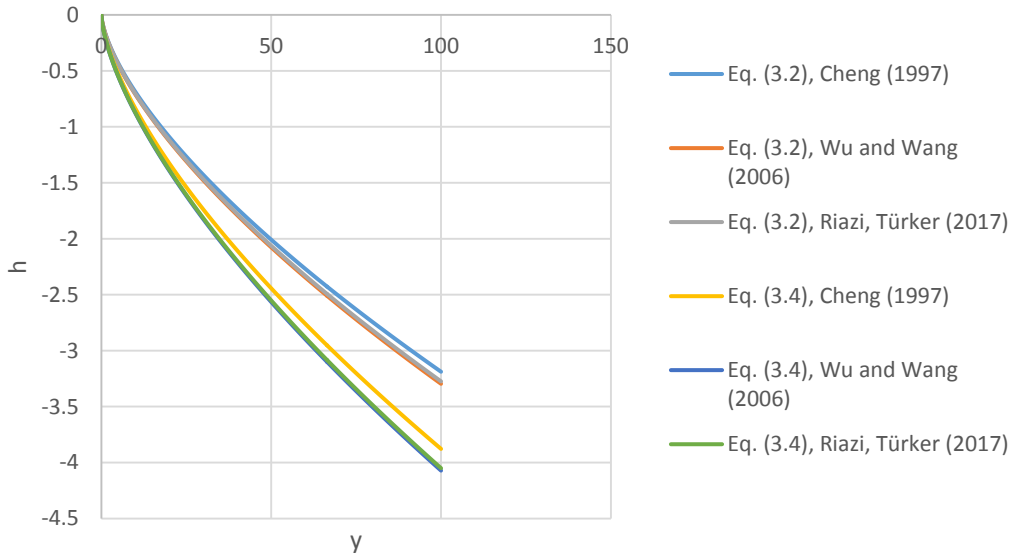

Figure 3.4: Effect of different particle settling velocity on EBP

As it can be observed in Fig. 3.4 different settling velocity equations don't have significant effect on estimating beach profiles. The same procedure has been done for particles with sizes ranging from 0.1mm up to 10mm and similarly no significant effect on estimating the beach profiles were observed. However, changing the approach from Eq. (3.2) to Eq. (3.4) has led to different beach profile. Therefore, although Eq. (3.22)

has improved the settling velocity estimations, the profile scale factor estimations through particle settling velocity has not been improved. It seems necessary to verify that the difference between an actual and an estimated equilibrium beach profile is due to the limitations in the equilibrium beach profile methodology, or the identified profile is out of equilibrium.

3.6 Best fit profile scale factor

Because of the low accuracy of the proposed profile scale factors, normally researchers obtain the magnitude of *A* through best fit process. In the best fit process it is assumed that the EBP is available. Accepting that Dean's (1977) approach presents the standard equilibrium beach profile shape (Wang and Kraus, 2005), in the best fit process, it is altered to an optimization problem with two unknowns:

$$h(y) = Ay^b \tag{3.25}$$

where the aim is to find best values for *A* and *b* that fits Eq. (3.25) to the EBP with the lowest error. Normally the values are obtained through a trial and error process. To improve the optimization process, a novel genetic algorithm was developed by Riazi and Türker (2017b). The best fit method has been compared with the new optimization method through five EBPs cited by Bodge (1992). The five EBPs are illustrated in Fig. 3.5.

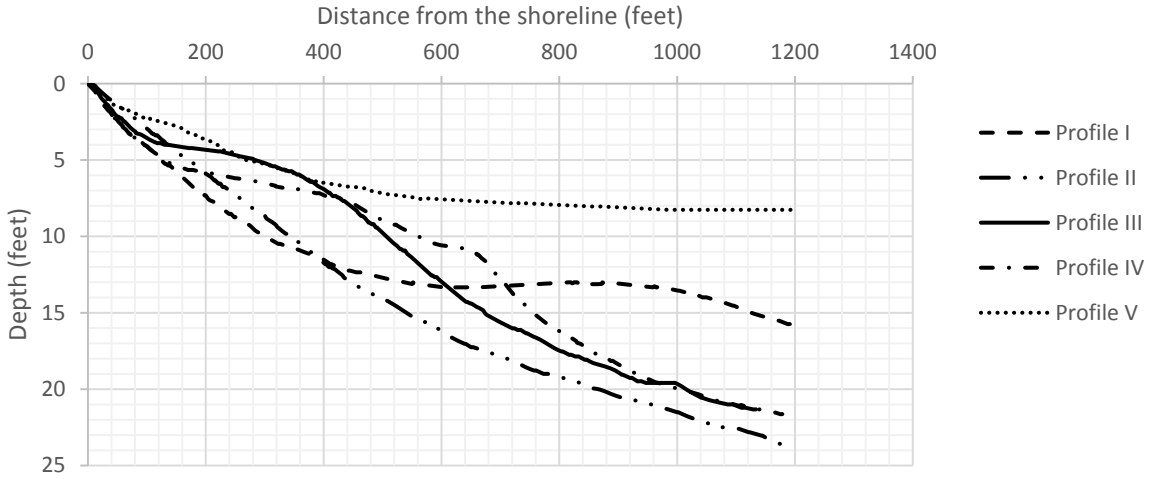

Figure 3.5: Five different EBPs from literature (Bodge, 1992).

The accuracy of the methods are compared through Mean Absolute Error (MAE), where the lower values of MAE indicates higher accuracy.

$$MAE = \frac{\sum_{i=1}^{n} |h(y_i)_{cal} - h(y_i)_{act}|}{n} \tag{3.26}$$

where n is the number of measured points in a profile, h_{cal} is the calculated depth by Eq. (3.17), and h_{act} is the actual measured depth of the profile at the distance of y.

The results obtained here are compared with the results proposed by Bodge (1992). As it is illustrated in Table 3.3, for all five profiles, the profile scale factors obtained by the method proposed by Riazi and Türker (2017b) have higher degree of accuracy with a lower mean absolute error.

Table 3.3: Comparison between the profile scale factor values obtained through the method proposed by Riazi and Türker (2017b) with the values obtained by best fit process that where cited by Bodge (1992).

Profile	n	Bodge (1992)			Proposed method		
		A ($ft^{1/3}$)	b	MAE (%)	A ($ft^{1/3}$)	b	MAE (%)
I	191	1.035	0.385	105.3	1.045	0.382	104.8
II	201	0.167	0.706	73.5	0.137	0.735	71.6
III	195	0.036	0.914	85.5	0.024	0.975	83.8
IV	160	0.037	0.905	98.1	0.031	0.932	97.8
V	217	0.474	0.419	58.00	0.657	0.363	40.1

Although best fit method can be used to obtain more accurate profile shape estimations, it has three main disadvantages. First, the best fit method for the calculation of *A* is based on the assumption that beach profiles are available and are in equilibrium condition. Second, in most cases the location of depth of closure in beach profiles obtained based on the best fit *A* differs from those in actual profiles. As the depth of closure depends on the wave climate and sediment diameter, the profile obtained through best fit method refers to a profile with different wave climate and sediment diameter distribution. Third, in the best fit method the analytical value 2/3 for *b* is changed to an empirical value.

There are adequate theoretical and experimental evidences to show that Dean's (1977) approach can be improved to estimate accurate EBPs. However, for instance, the errors obtained in Table 3.3 are not satisfactory. It should be noted that Dean's (1977) approach is based on the assumption that the profile is in equilibrium condition. Hence, the errors can be due to beach profile condition, where the equilibrium condition may have not been reached yet. Therefore, it seems necessary to propose a model that can be used to distinguish equilibrium from disequilibrium beach profiles.

Chapter 4

METHODOLOGY

4.1 Introduction

Thus far, among the methods of estimating the profile scale factor, best fit method has better accuracy. However, as it is illustrated in Table 3.2, the profiles estimated through best fit *A*, have an error ranging between %40 to 105%. Obtained error could be due to the limitation of the proposed approaches or simply, the specified profile can be out of equilibrium condition. Accepting Dean's (1977) theoretical approach, it seems necessary to be able to check if a profile has reached its equilibrium condition or not.

To this aim, considering the destructive forces as the main cause of erosion and constructive forces as the main cause of accretion, herein, the definition that defines the EBPs as the balance between the amount of erosion and accretion is employed. Hence, the amount of erosion and accretion forming a beach profile is used to declare that if a profile has reached its equilibrium condition. Therefore, as proposed by Riazi and Türker (2017a), first, the initial beach profile is required. The initial beach profile is defined as the primary shape of a profile in absence of destructive forces, mainly waves. The advantage of having the initial beach profile is that the amount of erosion and accretion causing the initial profile to transform to its current shape can be calculated. In order to be able to find the initial beach profile, herein, a boundary based profile scale factor is introduced. In a normalized coordinate system, the proposed boundary

based profile scale factor determines a turning point on the profile that demarcates the erosion from accretion area. It will be analytically shown that permanently the turning point in all EBPs will be equal to a fixed constant number. Therefore, the value of the turning point will be a good evidence to distinguish equilibrium from non-equilibrium beach profiles.

In the interest of the validity of the proposed approach, sixteen different groups of beach profiles from the literature has been employed. They all have been claimed that are in equilibrium condition. As illustrated in Table 4.1 the profiles have been gathered from three well-known previously published research articles. The groups are ten EBPs (group I to X) investigated by Dean (1977) and cited by Bodge (1992), three EBPs (group XI to XIII) examined by Romanczyk et al. (2005), and three EBPs (XIV to XVI) studied by Zenkovich (1967) and cited by Dean (1991).

Table 4.1: Beach profiles as reported in the literature and claimed to be in equilibrium condition. The best fit *A* is calculated by the mentioned researchers and fits Eq. (3.1) to the profiles with the lowest error.

Group	Location	Country	Sea	Best fit A ($m^{1/3}$)
	Bodge 1992			
I	From Montauk Point To Rockaway Beach	USA	Atlantic ocean	0.107
II	From Sandy Hook To Cape May	USA	Atlantic ocean	0.146
III	From Fenwick Light To Ocean City Inlet	USA	Atlantic ocean	0.127
IV	From Virginia Beach To Ocracoke	USA	Atlantic ocean	0.122
V	From Folly Beach To Tybee Island	USA	Atlantic ocean	0.061
VI	From Nassau Sound To Golden Beach	USA	Atlantic ocean	0.105
VII	Key West	USA	Gulf of Mexico	0.038
VIII	From Caxambas Pass To Clearwater Beach	USA	Gulf of Mexico	0.084
IX	From St. Andrew Pt. To Rollover Fish Pass	USA	Gulf of Mexico	0.063

Table 4.1: continued.

Group	Location	Country	Sea	Best fit A ($m^{1/3}$)
X	From Galveston To Brazon Santiago	USA	Gulf of Mexico	0.067
	Romańczyk et al. 2005			
XI	Queensland	Australia	Coral Sea	0.143
XII	North Carolina	USA	Atlantic Ocean	0.095
XIII	Jerba Island	Tunisia	Mediterranean Sea	0.063
	Dean 1991			
XIV	Kamchatka	Russia	Pacific Ocean	0.82
XV	Krasnodar Krai	Russia	Black Sea	0.25
XVI	Kamchatka	Russia	Pacific Ocean	0.07

In Table 4.1 equilibrium beach profiles categorized as Group I to Group X are the average profile of 35, 43, 38, 29, 15, 234, 10, 35, 38, and 27 measured profiles, respectively. The beach sediment in Group XI is silica sand with diameter within the range of [0.2mm, 0.3mm]. The largest wave heights are measured 8.5-12m with corresponding wave periods of 14–22 seconds. In Group XII, the beach sediments in the nearshore zone are well sorted and composed of fine sand with diameters ranging from 0.11 to 0.21 mm. The beach sediment of Group XIII is composed of silica with a mean diameter of 0.2 mm and of carbonates with mean diameters of 0.08 mm. The wave climate, which is typical for the Southern part of the Mediterranean Sea, is comprised of waves with periods up to 14 s and corresponding wave heights of 3.5 m. Group XIV is a boulder coast with average sand diameter from 150 mm to 300 mm. The average sand diameter in Group XVI is 0.25 mm. The equilibrium beach profiles of the coastal regions mentioned in Table 4.1 are presented in Appendix B.

In this chapter, first the boundary based beach profile scale factor will be defined and later, the proposed profile scale factor will be used to define the turning point.

4.2 Boundary based beach profile scale factor

As it was mentioned in section 3.2.1 the profile scale factor expression proposed by Dean (1977) is a function of particle diameter. In any wave dominant beach, the diameter of sediments on the beach profile varies from shoreline to the offshore (Larson, 1991). Hence, defining the profile scale factor as a function of constant sediment diameter or particle settling velocity is an oversimplification that affects the accuracy of the profile estimations. In the interest of accuracy, it is essential to define the profile scale factor as a function of all parameters causing the shape of the profile. However, defining all parameters affecting the shape of a profile, yet may be impossible. Hence, a parameter that shows the resultant effect of all variables should be considered. Analyzing the water depth of sandy beaches over months and years shows considerable variation in the surf zone up to the point of closure where changes become imperceptible (Hallermeier, 1981). The concept of depth of closure is a fundamental cross-shore boundary condition for morphodynamics, beach nourishment, and sediment transportation. The location of depth of closure can be considered as the result of natural beach slope changes, incoming wave magnitudes, and the sediment diameter building the profile and it can be considered as the limit of the equilibrium beach profile (Dean, 2003). Therefore, herein, the profile scale factor A, is proposed in terms of depth of closure. Accordingly, in a 2D Cartesian coordinate system, the boundary points are considered as the shoreline with the coordinate of (0,0) and the depth of closure with the coordinate (y_c,h_c), where the water depth variations are negligible. Where, the distance from the shoreline, positive seaward (y), is considered as the horizontal axis and the vertical axis is defined as the depth of the water (h), positive downwards. Hence, in equilibrium condition, one can define the profile scale factor, A, such that Eq. (3.1) passes through the boundary coordinates.

$$A_c = h_c y_c^{-\frac{2}{3}} \tag{4.1}$$

where A_c is boundary based profile scale factor. Fig. 4.1 illustrates the difference between the estimated EBP for Group I through Eq. (4.1) and the best fit A obtained by previous researchers.

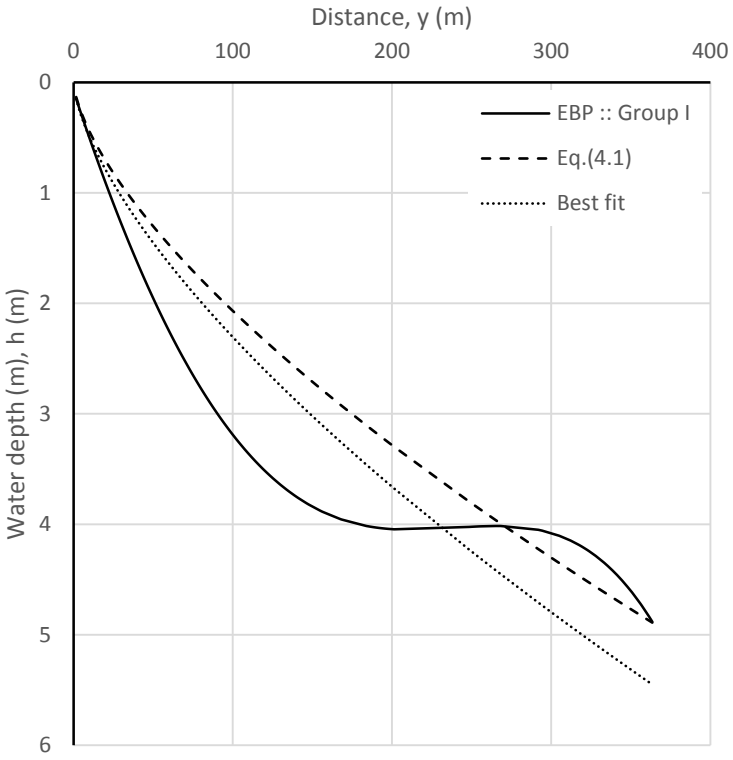

Figure 4.1: A model of natural EBP based on Dean's (1977) approach, illustrating proposed scale factor in contrast to the best fit A. As it can be observed Eq. (4.1) estimates a profile with the same depth of closure as the natural EBP.

As the change in the magnitude of the depth of closure exemplifies a new wave climate and a different sediment diameter distribution over the beach profile, the estimated profile through best fit A represents EBP with different natural conditions. The advantage of the proposed A_c, as shown in Fig. 4.1, is that the magnitude of estimated and natural depth of closure are equal, and therefore, at least it is estimating a profile with similar natural conditions.

4.3 Initial profile and the turning point

Without waves, the shape of a sandy beach will have a linear formation (Dean and Dalrymple, 2002). Considering the linear profile as the initial beach profile, the amount of erosion and accretion causing the initial linear profile to transform to the natural EBP can be defined. As illustrated in Fig. 4.2, by considering a local balance between the amount of erosion and accretion on the profile, a turning point can be defined that separates the erosion and accretion volume per unit width on the profile with respect to the initial linear profile.

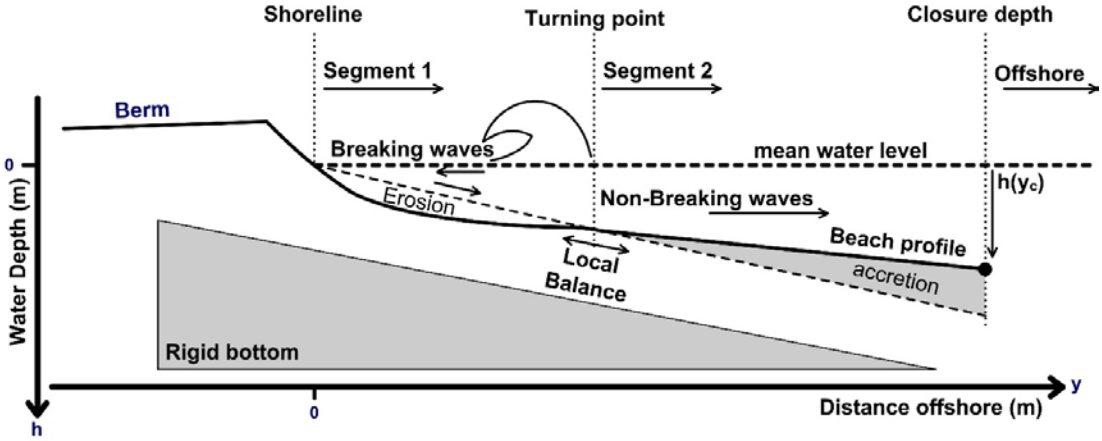

Figure 4.2: A sketch of equilibrium beach profile. The still-water depth is defined as a function of horizontal distance from the shoreline *h(y)* and local balance between the erosion and accretion volume per unit width on EBP. In this figure, the breaking waves are considered as the main cause of erosion

To have an applicable global model, in this study the effect of scale is omitted through a normalized coordinate system. To this end, to ensure that all beach profiles have theoretically common scale ranging within [0, 1], the distance from shoreline and the depth of water is normalized respectively through Eq. (4.2) and Eq. (4.3) by considering the coordinates of depth of closure as the end limit of EBP (Dean, 2003).

$$y^* = \frac{y_i}{y_c} \tag{4.2}$$

$$h^* = \frac{h_i}{h_c} \tag{4.3}$$

where y_i is the horizontal distance of a point within the profile to the origin of the profile, positive seawards; and h_i is the water depth positive downwards. The main advantage of normalized coordinate system is that the value of A_c calculated through Eq. (4.1) will always be equal to 1 and therefore, Eq. (3.1) in a normalized coordinate system will be independent of profile scale factor, *A*.

$$h^* = (y^*)^{\frac{2}{3}} \tag{4.4}$$

Considering the effect of sediment compression can be negligible, in an analytical approach, the amount of sediment eroded should be equal to the amount of sediment accreted. In this regard, in a normalized coordinate system, Eq. (4.4) leads to the definition of an initial linear beach profile and global turning point. To obtain the initial linear beach profile, the volume of water per unit width (α) above the profile is calculated (Fig. 4.3), bearing in mind that the water above the sand shapes the beach profile.

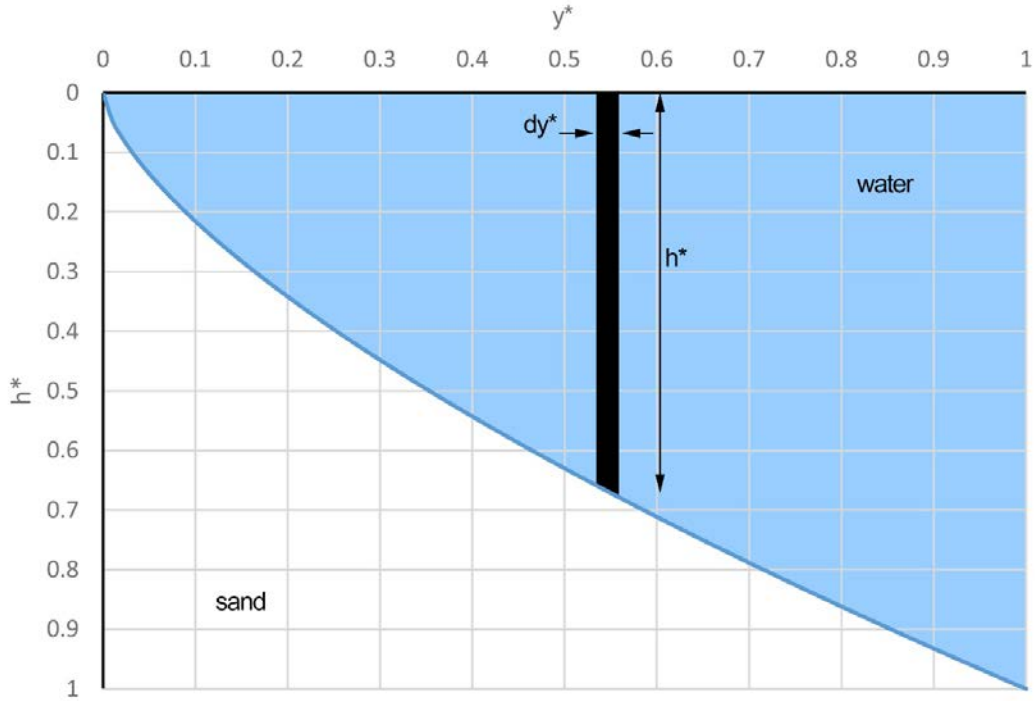

Figure 4.3: Representation of EBP through Eq. (4.4). The profile is the lower boundary for the volume of water per unit width above the sand. Given h^* as a function of y^*, the volume of water per unit width can be calculated by definite integral of y^* over the interval [0,1].

$$\alpha = \int_0^1 h^* \, dy^* \tag{4.5}$$

By solving Eq. (4.5) with respect to Eq. (4.4), the volume of water per unit width in a normalized coordinate system is equal to $\alpha = 0.6 \frac{m^3/m}{m^3/m}$. Considering the absence of wave, the water and the sand in the profile should be linearly equipoised. Therefore, by keeping the offshore distance constant, the calculated volume of water per unit width ($0.6 \frac{m^3/m}{m^3/m}$) is reshaped as a right triangle so that the profile will have a linear shape (Fig. 4.4). The obtained linear line (hypotenuse of the right triangle) that separates the water and sand making the beach is considered as the initial linear beach profile. Since the offshore distance is constant the same amount of volume of water above the beach profile ($0.6 \frac{m^3/m}{m^3/m}$) can be reached when $h^* = 1.2$. Therefore, the

equation of the initial linear beach profile can be obtained as:

$$h^* = 1.2y^* \tag{4.6}$$

In a normalized coordinate system Eq. (4.6) and Eq. (4.4) coincides at $y^* = 0.58$. As illustrated in Fig. 4.4, the evolution of changes from the initial linear profile, Eq. (4.6), to the final equilibrium beach profile, Eq. (4.4), can be divided into two parts. One is from the shoreline up to $y^* = 0.58$ that the destructive forces have caused erosion from the initial linear profile and the other from $y^* = 0.58$ to depth of closure where the offshore sediment transport has formed accretion. Therefore, this point is considered as the turning point. As the EBPs are completely different from beach to beach, the corresponding value of h^* when $y^* = 0.58$ differs for different profiles.

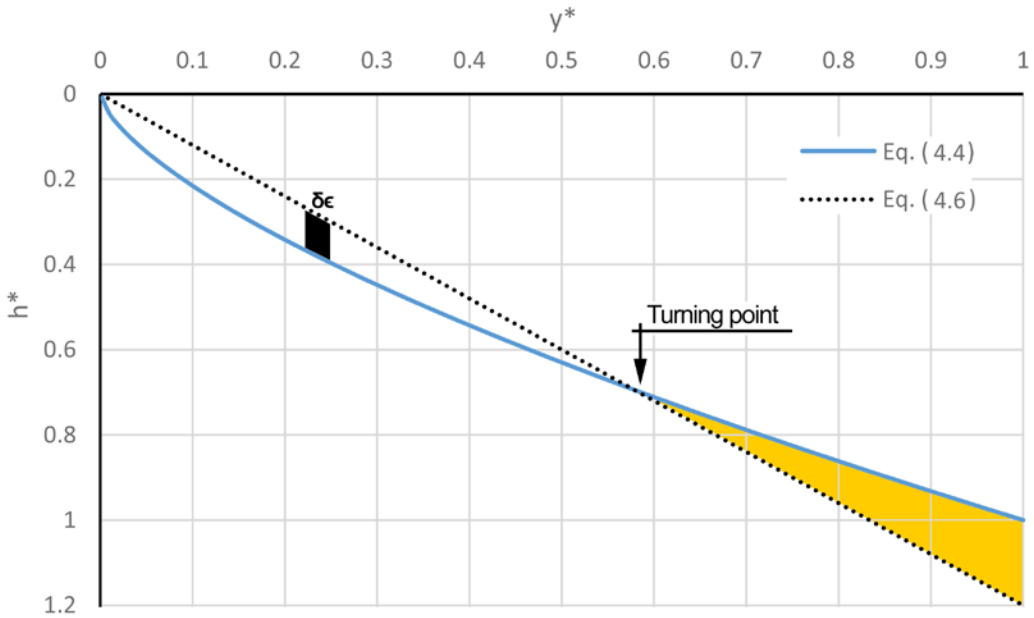

Figure 4.4: Initial linear and analytical representation of natural equilibrium beach profiles in a normalized coordinate system. The empty space between the initial linear profile and EBP up to the turning point illustrates the amount of erosion required so that the initial linear profile transforms into the analytical representation of natural equilibrium profile.

The advantage of Figure 4.4 is that the amount of erosion and accretion causing the initial linear beach profile to transform to the equilibrium condition can be calculated. Thus, the volume per unit width of the erosion can be defined as:

$$\delta\epsilon = dh^* \times dy^* \tag{4.7}$$

Eq. (4.7) can be used to calculate the exact volume of erosion per unit width in contrast to the initial linear profile in an analytical equilibrium beach profile:

$$\begin{aligned} Erosion &= \int_0^{0.58} \left(y^{*\frac{2}{3}} - 1.2y^* \right) dy^* \\ &= 0.04 \ \frac{m^3/m}{m^3/m} \end{aligned} \tag{4.8}$$

Consequently, with the same concept the volume per unit width of the accretion can be calculated.

$$\begin{aligned} Accretion &= \int_{0.58}^{1} \left(1.2y^* - y^{*\frac{2}{3}} \right) dy^* \\ &= 0.04 \ \frac{m^3/m}{m^3/m} \end{aligned} \tag{4.9}$$

Since the normalized volume per unit width of erosion and accretion are equal, results of Eq. (4.8) and Eq. (4.9) provide evidence that the beach is in equilibrium condition. This process can be applied to beach profiles to validate if the profiles are in an equilibrium state.

Chapter 5

RESULTS AND DISCUSSIONS

This chapter presents the results and discussion of the methods, that is, the boundary based profile scale factor and the turning point as presented in Chapter 4. In order to assess the applicability of the model, the model is exposed to different wave climates and mean morphologies. First, the proposed boundary based profile scale factor, Eq. (4.1), is validated in section 5.1. Next, the reliability of the proposed turning point is discussed in section 5.2.

5.1 Validity of the boundary based profile scale factor

The proposed boundary based profile scale factor, is validated through the previously confirmed equilibrium beach profiles defined in Table 4.1. As it is illustrated in Table 5.1 the relative error among the "Best fit *A*" obtained by other researchers and proposed boundary based *A* is calculated.

As it can be seen in Table 5.1, Eq. (4.1) is able to calculate the value of *A* with an average relative error of 8.14%. The proposed boundary based profile scale factor is based on the fact that the estimated and natural EBPs should have the same depth of closure. It can, therefore, be seen that in profiles such as Group XIV where the best fit *A* obeys the same rule (Fig. 5.1: Group XIV), the error of calculated *A* decreases enormously. However, when the beach profile plotted based on best fit *A* takes a different depth of closure (Fig. 5.1: Group XVI), the error of *A* calculated through Eq. (4.1) increases. Accepting that the depth of closure defines the offshore limits of EBPs, the relative error obtained in Table 5.1 shows the vertical deviation of depth of closure

plotted by the help of best fit *A*. As depth of closure variation depends on changes in wave climate and different sediment diameter distribution, the relative error illustrates the inaccuracy of best fit *A*.

Table 5.1: Relative error of the proposed profile scale factor. Lower relative errors indicate that the predictions of *A* by Eq. (4.1) are close to the values obtained through best fit process.

Group	Best fit *A*	Boundary Based *A*	Relative error (%)	Comment
I	0.107	0.096	10.28	Underestimation
II	0.146	0.143	2.05	Underestimation
III	0.127	0.132	3.94	Overestimation
IV	0.122	0.130	6.56	Overestimation
V	0.061	0.049	19.67	Underestimation
VI	0.105	0.106	0.95	Overestimation
VII	0.038	0.041	7.89	Overestimation
VIII	0.084	0.072	14.29	Underestimation
IX	0.063	0.057	9.52	Underestimation
X	0.067	0.065	2.99	Underestimation
XI	0.143	0.159	11.19	Overestimation
XII	0.095	0.091	4.21	Underestimation
XIII	0.063	0.069	9.52	Overestimation
XIV	0.82	0.821	0.12	Overestimation
XV	0.25	0.236	5.60	Underestimation
XVI	0.07	0.085	21.43	Overestimation
Minimum			0.12	
Average			8.14	
Maximum			21.43	

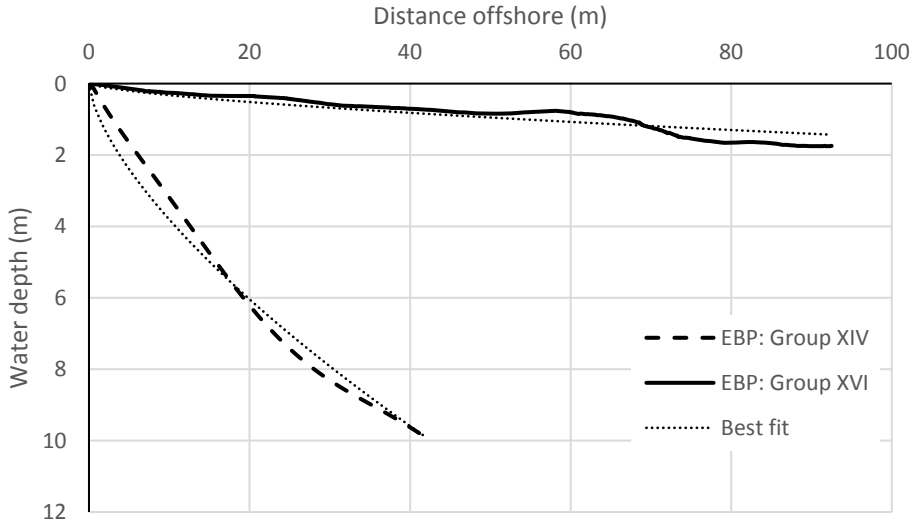

Figure 5.1: Equilibrium beach profiles XIV and XVI with predicted profiles in previous studies with lowest and highest diverse to depth of closure, respectively.

The profile scale factor related to equilibrium profile XIV with the magnitude of $0.8m^{1/3}$ falls beyond the average value of profile scale factors mentioned in Table 4.1. The main reason for this observation is that the depth of closure with the magnitude of 9.9 meter happens at 41.6 meter away from the shoreline. The high slope of the profile causes the profile scale factor to be enormously large.

5.2 Reliability of the proposed turning point

By applying the proposed model to all the 16 beach profiles mentioned in Table 4.1 the reliability of the turning point is obtained. For all the beach profiles the depth of closure is considered based on the one presented in the literature and as it is illustrated in Fig. 5.2 to 5.17, the profiles are normalized through Eqs. (4.2) and (4.3).

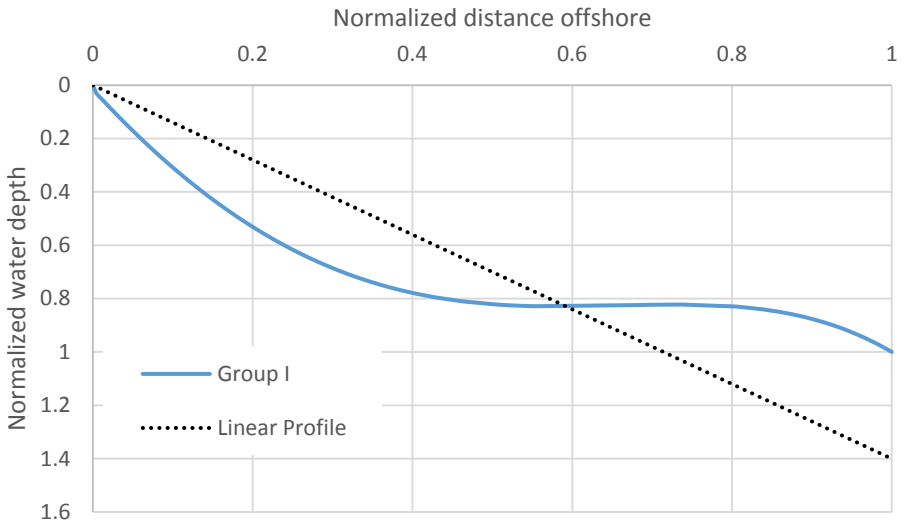

Figure 5.2: Coincide of the natural equilibrium beach profile, Group I, and its initial linear profile in a normalized coordinate system.

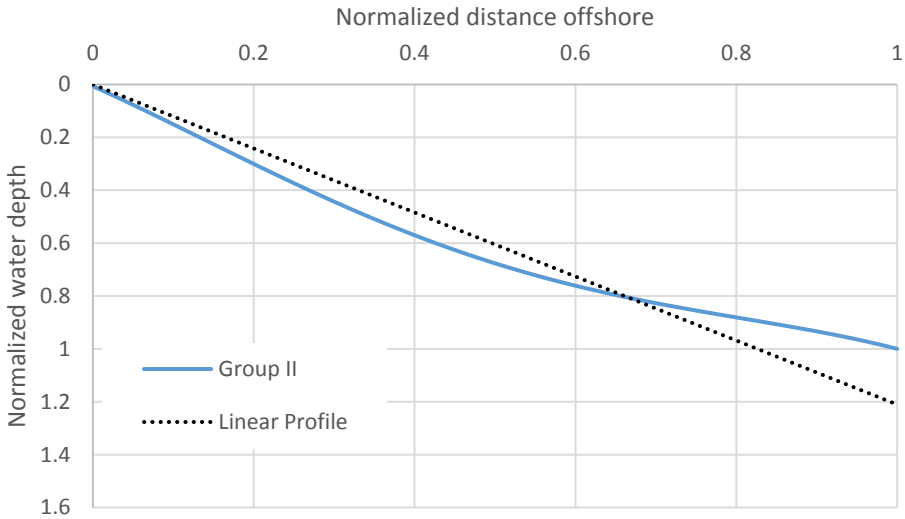

Figure 5.3: Coincide of the natural equilibrium beach profile, Group II, and its initial linear profile in a normalized coordinate system.

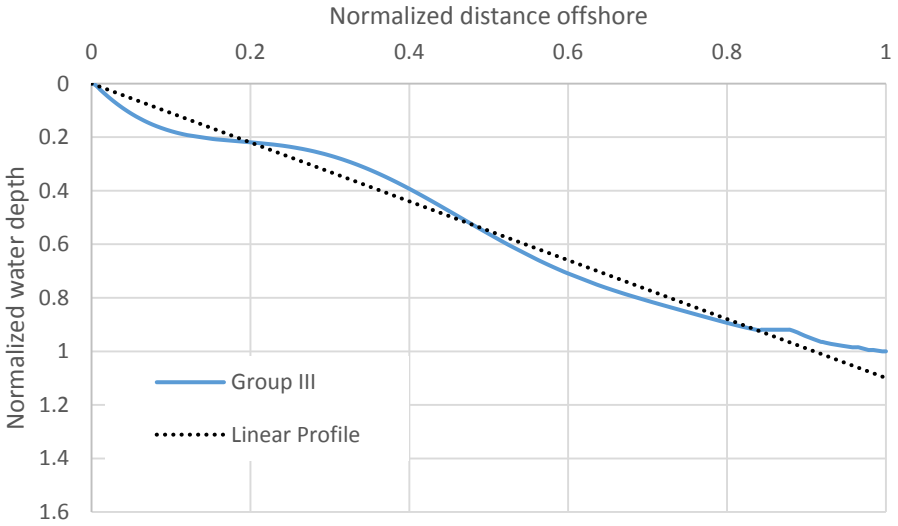

Figure 5.4: Coincide of the natural equilibrium beach profile, Group III, and its initial linear profile in a normalized coordinate system.

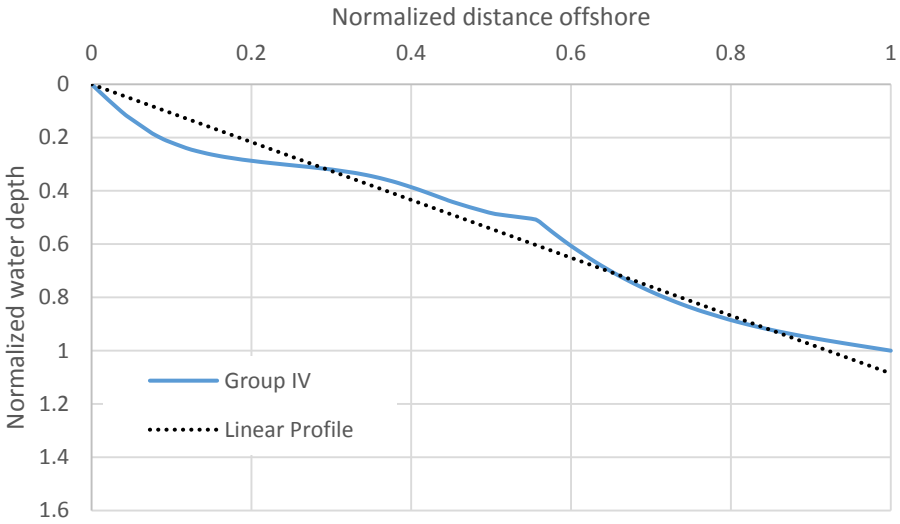

Figure 5.5: Coincide of the natural equilibrium beach profile, Group IV, and its initial linear profile in a normalized coordinate system.

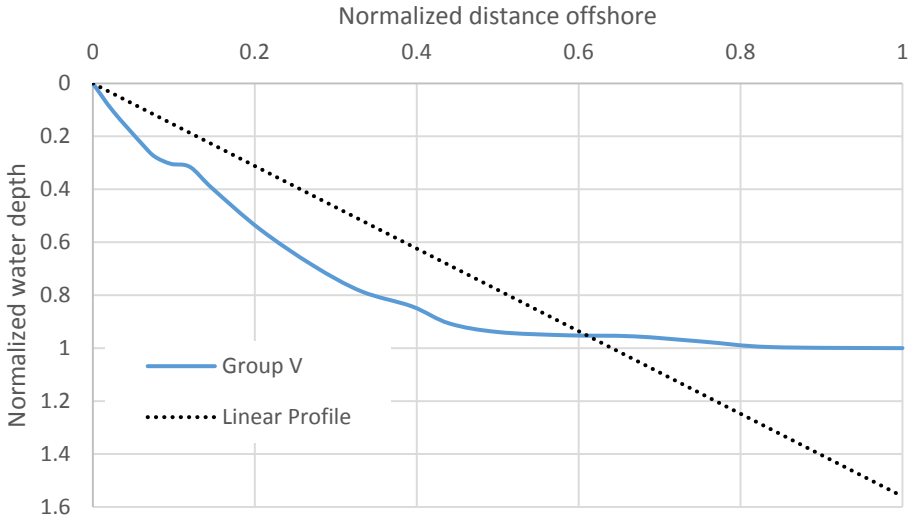

Figure 5.6: Coincide of the natural equilibrium beach profile, Group V, and its initial linear profile in a normalized coordinate system.

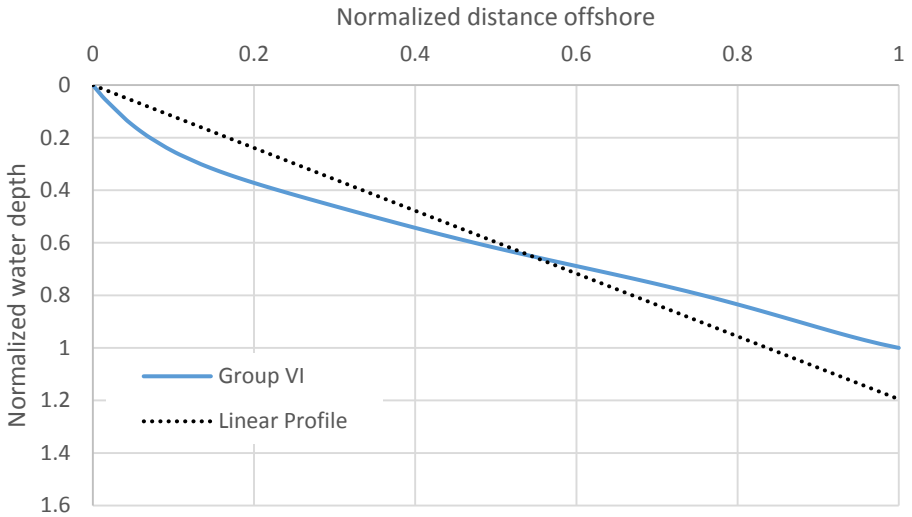

Figure 5.7: Coincide of the natural equilibrium beach profile, Group VI, and its initial linear profile in a normalized coordinate system.

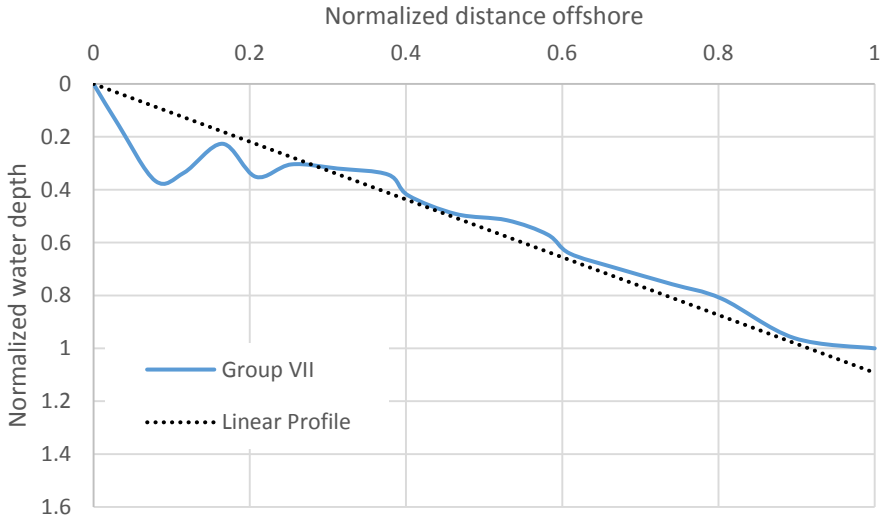

Figure 5.8: Coincide of the natural equilibrium beach profile, Group VII, and its initial linear profile in a normalized coordinate system.

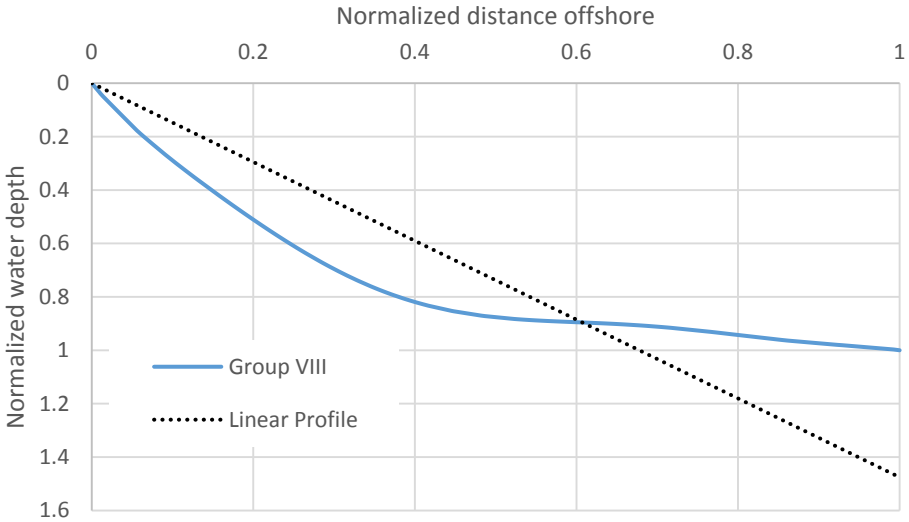

Figure 5.9: Coincide of the natural equilibrium beach profile, Group VIII, and its initial linear profile in a normalized coordinate system.

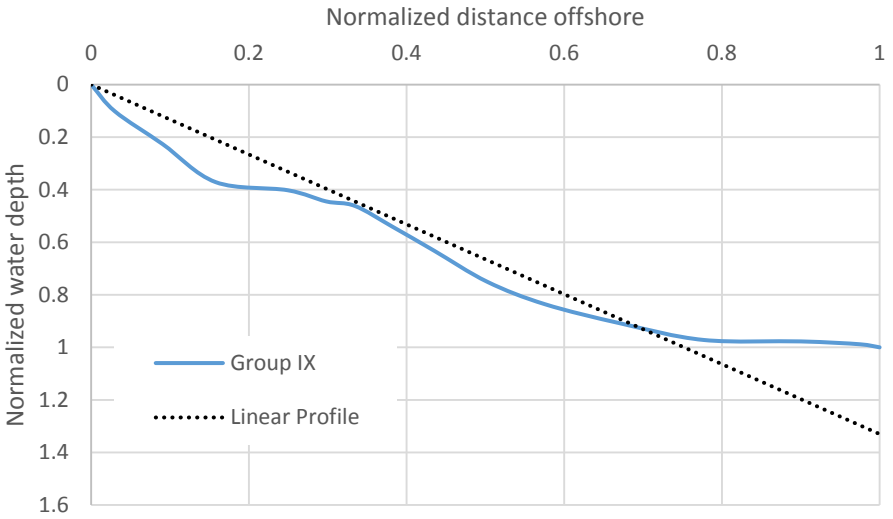

Figure 5.10: Coincide of the natural equilibrium beach profile, Group IX, and its initial linear profile in a normalized coordinate system.

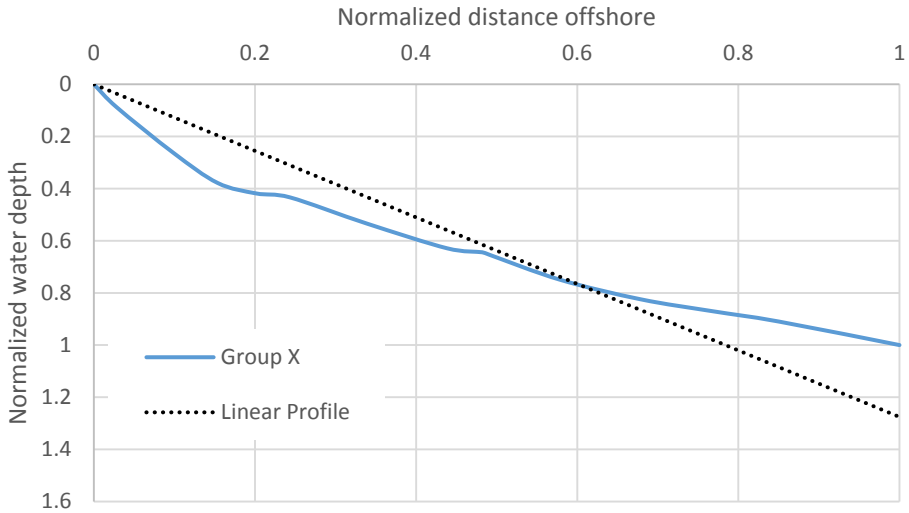

Figure 5.11: Coincide of the natural equilibrium beach profile, Group X, and its initial linear profile in a normalized coordinate system.

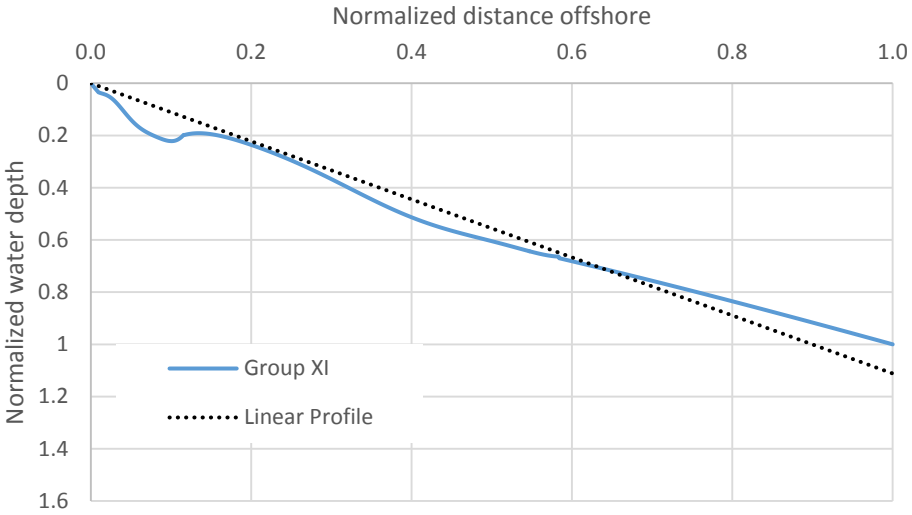

Figure 5.12: Coincide of the natural equilibrium beach profile, Group XI, and its initial linear profile in a normalized coordinate system.

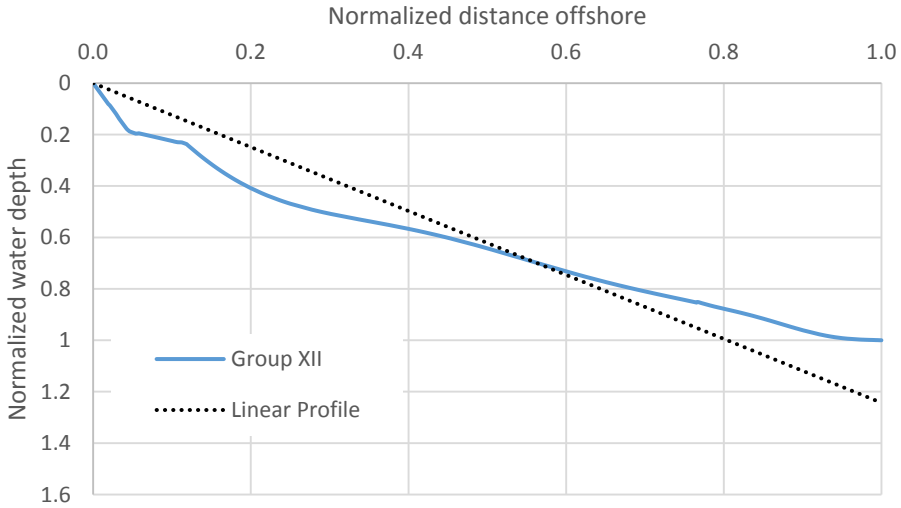

Figure 5.13: Coincide of the natural equilibrium beach profile, Group XII, and its initial linear profile in a normalized coordinate system.

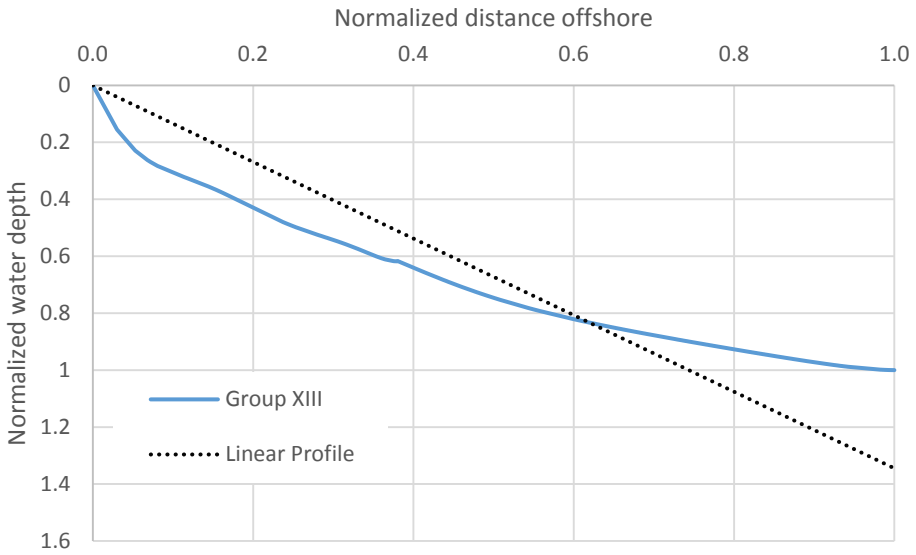

Figure 5.14: Coincide of the natural equilibrium beach profile, Group XIII, and its initial linear profile in a normalized coordinate system.

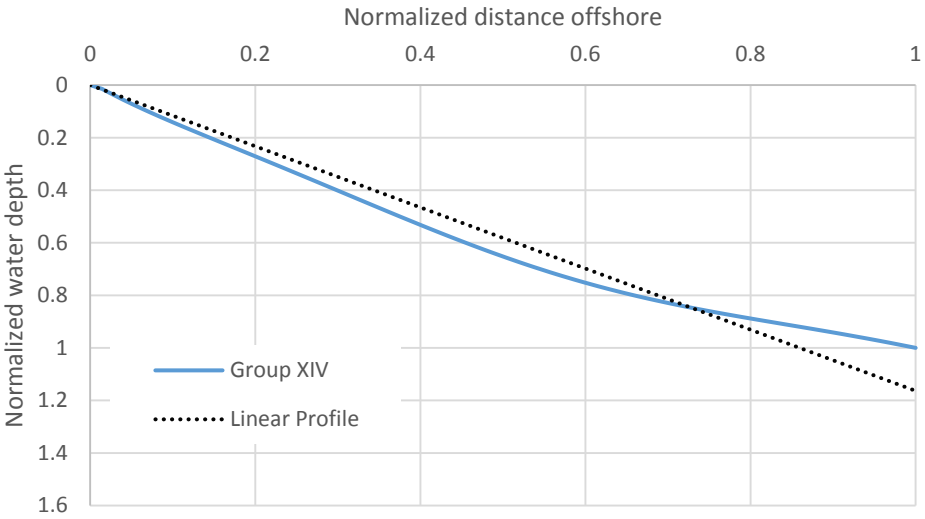

Figure 5.15: Coincide of the natural equilibrium beach profile, Group XIV, and its initial linear profile in a normalized coordinate system.

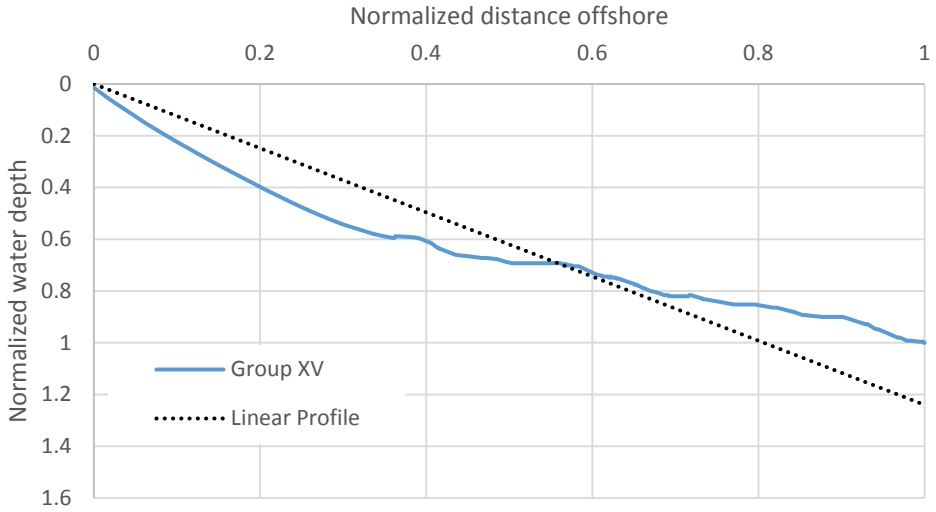

Figure 5.16: Coincide of the natural equilibrium beach profile, Group XV, and its initial linear profile in a normalized coordinate system.

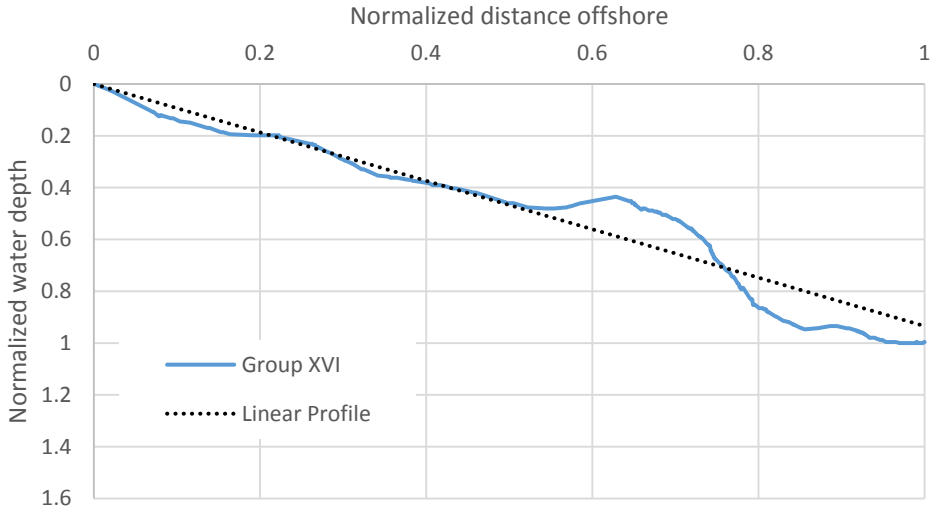

Figure 5.17: Coincide of the natural equilibrium beach profile, Group XVI, and its initial linear profile in a normalized coordinate system.

Based on Figs. 5.2 to 5.17 the amount of normalized erosion and accretion of all 16 beach profiles were calculated (Table 5.2).

Table 5.2: Results of the proposed model applied on the beach profiles employed from literature.

Group	Normalized volume of water per unit width	Normalized turning point	Normalized volume of erosion per unit width	Normalized volume of accretion per unit width
I	0.7001	0.59	0.1001	0.1024
II	0.6052	0.66	0.0309	0.0335
III	0.5498	0.2, 0.48, 0.84	0.0147	0.0154
IV	0.5427	0.28, 0.66, 0.84	0.0199	0.0194
V	0.7799	0.61	0.1018	0.1030
VI	0.5976	0.54	0.0428	0.0434
VII	0.5462	0.28	0.0324	0.0238
VIII	0.7377	0.6	0.1901	0.1816
IX	0.6583	0.7	0.0436	0.0447
X	0.6313	0.6	0.0248	0.0255
XI	0.5558	0.64	0.0247	0.0191
XII	0.6215	0.56	0.0490	0.0433
XIII	0.6724	0.62	0.0671	0.0592
XIV	0.5818	0.73	0.0284	0.0210
XV	0.6201	0.56	0.0590	0.0497
XVI	0.4672	0.205, 0.28, 0.42, 0.76	0.0302	0.0218

In section 4.3, it was analytically shown that in a beach profile when the value of the turning point is equal to 0.58 the amount of erosion and accretion will be equal to each other. As it can be observed in Table 5.2, practically, in all the beach profiles, when the turning point approaches to the analytical value of $y^{*}= 0.58$, the erosion and accretion values balance each other. Among all the profiles mentioned in Table 5.2, the highest error between the amount of erosion and accretion belongs to profiles VII, XIV, and XVI where the turning point has the highest variation. Furthermore, it appears that beach profiles III, IV, and XVI are more tended to possess multiple low-amplitude bars that usually occur on wide, flat, and low wave energy beaches (Short, 1991) where the formations are enforced by cross-shore standing long waves (Wijnberg and Kroon, 2002). By eliminating these three multiple bar profiles that cut the initial linear profile in more than one point, the average normalized turning point is equal to 0.59 with standard deviation of 0.104 and standard error (SE) equal to 0.029.

Based on the obtained SE and the average turning point, the lower and upper endpoints of the 95% confidence interval of the turning point is calculated through Eq. (5.1) and Eq. (5.2).

$$Lower\ endpoint\ =\ 0.59 - 1.96 \times SE\ =\ 0.53 \qquad (5.1)$$

$$Upper\ endpoint\ =\ 0.59 + 1.96 \times SE\ =\ 0.65 \qquad (5.2)$$

For the mentioned 13 beach profiles, the analytical value for the turning point (y^*=0.58) is covered by the 95% confidence interval ([0.53, 0.65]). This means that the desired value for the turning point will occur in the confidence interval stated at the 95% confidence level of another group of equilibrium beach profiles and provides evidence for reliability of the proposed model.

5.3 Practical use of the model for two Cyprus beaches

Moreover, the proposed model is applied to beach profiles gathered form two different locations in Cyprus. One located at the north coast with coordinates of 35°26'N 33°58'E (site A), and the other one located at the east coast of the island with the coordinates of 35°15'N 33°54'E (site B). The timewise average changes of beach profiles were not available. Therefore, only the beach profiles which were measured for different construction purposes are employed. The aim is to validate if the measured profiles have reached the equilibrium condition. The Google Earth pictures of the regions are given Fig. 5.18.

Figure 5.18: Google Earth images of the employed regions in Cyprus

In region A and B the profiles have been measured up to the distances of 580 meter and 64 meters from the shoreline, respectively. The profiles are illustrated in been Fig. 5.19 and 5.20.

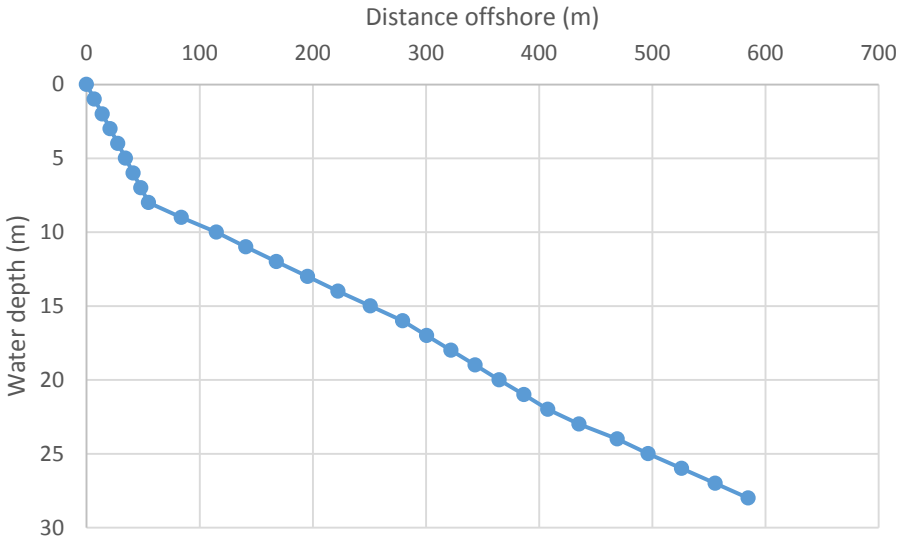

Figure 5.19: Site A, Kaplıca: measured profile

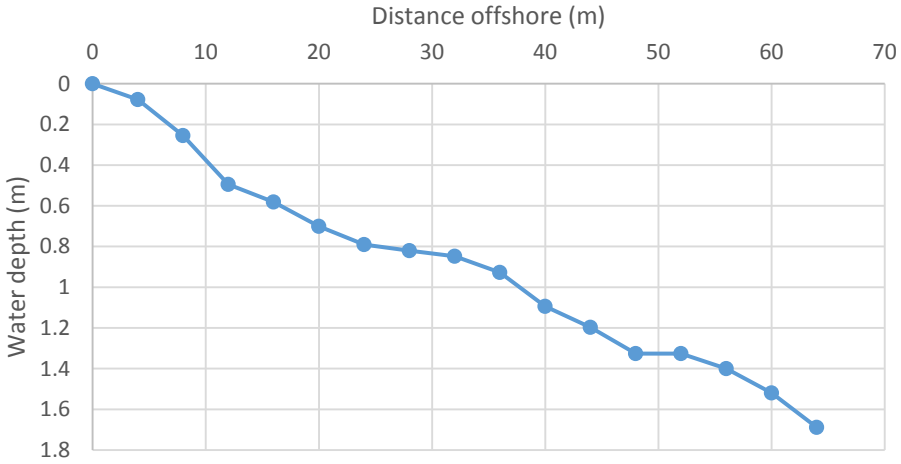

Figure 5.20: Site B, İskele: measured profile

The presented model is applied to the measured beach profiles to check if the profiles are equilibrium condition. As it can be observed in Fig 5.21 and Fig. 5.22 the turning point in beach profile region A is equal to 0.5 and in beach profile region B is equal to 0.4. The amount of Normalized volume of erosion and accretion per unit width is given in Table 5.3.

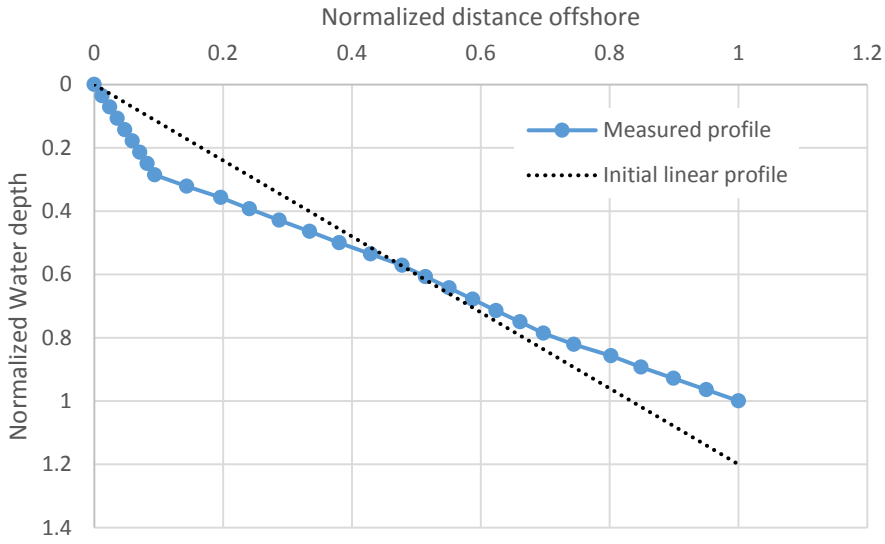

Figure 5.21: Site A, Kaplıca: normalized beach profile and its linear initial profile.

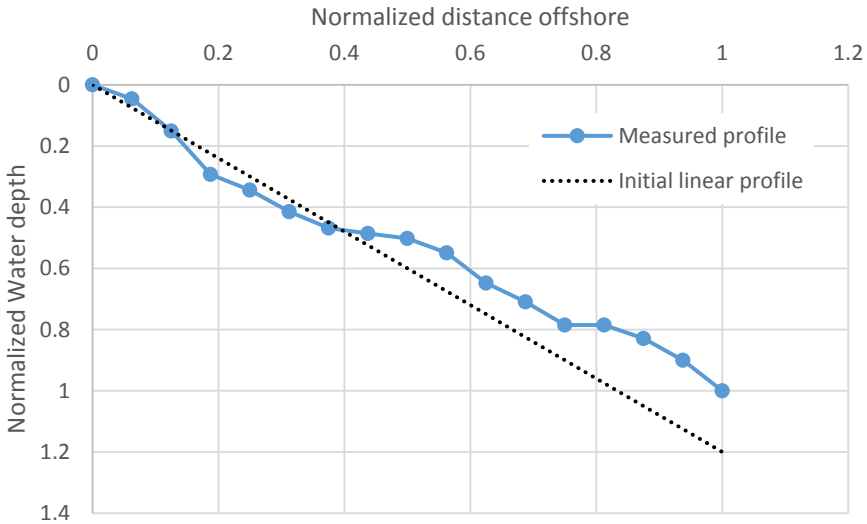

Figure 5.22: Site B, İskele: normalized beach profile and its linear initial profile.

Table 5.3: Three different beach profiles measured and tested at coasts of Cyprus.

Site	Region	Turning point	Normalized volume of erosion per unit width	Normalized volume of accretion per unit width
A	Kaplıca	0.5	0.071	0.088
B	İskele	0.4	0.024	0.138

As it can be seen in Table 5.3 when the value of turning point is close to the analytical value of 0.58, the amount of erosion and accretion balance each other. Between

the two profiles from site A and B, clearly the profile in site B is out of equilibrium and the profile in site A can roughly be considered to be in equilibrium.

Chapter 6

CONCLUSION

6.1 Conclusions

Estimating the profile scale factor, *A*, that is a function of wave energy dissipation is a complex task. Therefore, researchers have tried to estimate the value of *A*, through easily accessible parameters such as particle settling velocity. Hence, in this study, first the particle settling velocity was investigated comprehensively. It was realized that a new and novel approach can be proposed that will lead to better estimations of particle settling velocity. In this process, an optimizing method was required. To this aim, through genetic algorithm, a new model has been proposed that can optimize engineering problems with higher degree of accuracy. The new optimization model was applied to the novel settling velocity approach and a new equation for the estimation of the particle settling velocity was developed and proposed. The new settling velocity equation was employed and compared with other settling velocities presented in the literature and it was observed that it can be used to improve the estimations of profile scale factor. However, the amount of improvement was not satisfactory. As it is stated in literature, the magnitude of *A* can be estimated with the highest accuracy through a best fit process. However, the main disadvantage of the best fit process is that the assumption which the beach profile is in equilibrium condition is not verified. To overcome the mentioned disadvantage, a boundary based *A* was proposed. Through the proposed *A*, in a normalized coordinate system a global unique solution for EBPs was obtained. Then the unique solution was used to define a turning point that separates

the erosion from accretion area. The balance between the amount of erosion and accretion was employed to check if a certain profile is in equilibrium condition or not. In order to assess the applicability of the model, it was applied to different wave climates and mean morphologies. The results provided evidence for the validity and accuracy of the proposed profile scale factor. In addition, using a 95% confidence interval, it was shown that the proposed turning point is reliable as well.

6.2 Recommendations for future studies

This study was conducted to improve the definition of equilibrium beach profiles. Hence, it is recommended to recheck previous studies that involve EBPs to validate if all the employed profiles were in equilibrium condition and if not, to check and see if removing the non-equilibrium profiles will affect the obtained results. Moreover, the model was applied on a distance from shoreline to offshore. It is recommended to test the model for the portion before the shoreline. Furthermore, in regards to profile shape factor, available equations for estimating the depth of closure can be employed and combined with the proposed boundary based profile shape factor.

REFERENCES

Aragonés, L., Serra, J. C., Villacampa, Y., Saval, J. M., & Tinoco, H. (2016). New methodology for describing the equilibrium beach profile applied to the Valencia's beaches. *Geomorphology*, 259, 1-11.

Are, F., & Reimnitz, E. (2008). The A and m coefficients in the Bruun/Dean equilibrium profile equation seen from the Arctic. *Journal of Coastal Research*, 24(sp2), 243-249.

Bodge, K.R. (1992). Representing equilibrium beach profiles with an exponential expression. . *Journal of Coastal Research*, 8 (1), 47– 55.

Boon, J. D., & Green, M. O. (1989). Caribbean beach-face slopes and beach equilibrium profiles. *Coastal Engineering* , 1618-1630.

Bruun, P. (1954). Coast erosion and the development of beach profiles. Technical Memorandum No. 44, Beach Erosion Board, US Army Corps of Engineers, Waterways Experiment Station, Vicksburg, MS.

Camenen, B. (2007). Simple and General Formula for the Settling Velocity of Particles. *Journal of Hydrologic Engineering*, 133:2(229), 229-233.

CERC, (1984). Shore protection manual, 4th Edition. U.S. Army Engineer Waterway Experiment Station, Coastal Engineering Research Center, US Government Printing Office, Washington DC, USA.

Cheng, N. S. (1997). Simplified settling velocity formula for sediment particle. *Journal of Hydraulic Engineering*, 123(2), 149-152.

Choi, J., Roh, M., & Kim, Y. T. (2016). A Laboratory Experiment on beach profile evolution induced by two wave conditions dominated in the Haeundae Coast of Korea. *Journal of Coastal Research*, 75(sp1), 1327-1331.

Davidson-Arnott, R. (2010). Introduction to coastal processes and geomorphology. Cambridge University Press.

Dai, Z. J., Du, J. Z., Li, C. C., & Chen, Z. S. (2007). The configuration of equilibrium beach profile in South China. *Geomorphology*, 86(3), 441-454.

da Silva, P. A., Temperville, A., & Santos, F. S. (2006). Sand transport under combined current and wave conditions: A semi-unsteady, practical model. *Coastal Engineering*, 53(11), 897-913.

Dean, R.G. (1991). Equilibrium Beach Profiles: Characteristics and Applications. *Journal of Coastal Research*, 7, 53–84.

Dean, R. G., & Dalrymple, R. A. (2004). Coastal processes with engineering applications. Cambridge University Press.

DHL, (1970). Gold Coast, Queensland Australia — coastal erosion and related problems. Tech. Rep. R257, vol. 1–2. Delft Hydraulics Laboratory, Delft, Netherlands.

Dubois, R. N. (1999). An inverse relationship between the A and m coefficients in the Bruun/Dean equilibrium profile equation. *Journal of Coastal Research*, 186-197.

Hanson, H., & Kraus, N.C. (1989). GENESIS: generalized model for simulating change, Report 1: reference manual and user guide. Technical Report CERC, U.S. Army Engineer Waterways Experimental Station, Coastal Engineer Research Center, Vicksburg, Mississippi, pp. 19–89.

Hartman, M., & Kennedy, A. B. (2016). Depth of closure over large regions using airborne bathymetric lidar. *Marine Geology*, 379, 52-63.

Heward, A.P. (1981). A review of wave-dominated elastic shoreline deposits. *Earth-Science Reviews*, 17,pp. 223-276.

Julien, P. Y. (1995). Erosion and deposition. Cambridge University Press, Cambridge, U.K.

Kaiser, M. F. M., & Frihy, O. E. (2009). Validity of the equilibrium beach profiles: Nile delta coastal zone, Egypt. *Geomorphology*, 107(1), 25-31.

Komar, P.D., (1998). Beach Processes and Sedimentation, Second Edition. Prentice-Hall, Inc., New Jersey. 544 pp.

Komar, P.D., & McDougal, W.G., (1994). The analysis of exponential beach profiles. *Journal of Coastal Research,* 10 (1), 59– 69.

KomarP.D., & Reimers C.E. (1978). Grain shape effects on settling rates. *Journal of Geology*, 86(2) 193-209.

Kriebel, D. L., Kraus, N. C., & Larson, M. (1991). Engineering methods for predicting beach profile response. *Coastal Sediments (ASCE)*, 557-571.

Larson, M. (1991). Equilibrium profile of a beach with varying grain size. Proceedings of *Coastal Sediments (ASCE)*, 27, 905–919.

Ludka, B. C., Guza, R. T., O'Reilly, W. C., & Yates, M. L. (2015). Field evidence of beach profile evolution toward equilibrium. *Journal of Geophysical Research: Oceans*, 120(11), 7574-7597.

Masselink, G., Hughes, M., & Knight, J. (2014). Introduction to coastal processes and geomorphology. Routledge.

Masselink, G., & Short, A. D. (1993). The effect of tide range on beach morphodynamics and morphology: a conceptual beach model. *Journal of Coastal Research*, 785-800.

McArdle, S. B., & McLachlan, A. (1992). Sand beach ecology: swash features relevant to the macrofauna. *Journal of Coastal Research*, 398-407.

Moore, B.D. (1982). Beach Profile Evolution in Response to Change in Water Level and Wave Height MSc Thesis Department of Civil Engineering, University of Delaware.

Pilkey, O. H., Young, R. S., Riggs, S. R., Smith, A. S., Wu, H., & Pilkey, W. D. (1993). The concept of shoreface profile of equilibrium: a critical review. *Journal of Coastal Research*, 255-278.

Riazi, A., & Türker, U. (2017a). Equilibrium beach profiles: erosion and accretion balanced approach. *Water and Environment Journal*.

Riazi A., & Türker, U. (2017b). A Genetic Algorithm based search space splitting pattern and its application in hydraulic and coastal engineering problems. *Neural Computing and Applications.*

Riazi A., & Türker U. (2017c). The Drag Coefficient and Settling Velocity of Natural Silica Sands. Under review.

Romańczyk, W., Boczar-Karakiewicz, B., & Bona, J. L. (2005). Extended equilibrium beach profiles. *Coastal Engineering*, 52(9), 727-744.

She, K., Trim, L., & Pope, D. (2005). Fall velocities of natural sediment particles: a simple mathematical presentation of the fall velocity law. *Journal of Hydraulic Research*, 43(2), 189-195.

Short, A. D. (2005). Beaches of the Western Australian Coast: Eucla to Roebuck Bay: a Guide to Their Nature, Characteristics, Surf and Safety. Sydney University Press.

Short, A. D. (2000). Beaches of the Queensland Coast, Cooktown to Coolangatta: A Guide to Their Nature, Characteristics, Surf and Safety. Sydney University Press.

Smith D., & Cheung K. (2003). Settling Characteristics of Calcareous Sand. *Journal of Hydraulic Engineering*, 129(6) 479-483.

Swamee, P., & Ojha, C. (1991). Drag Coefficient and Fall Velocity of nonspherical particles. *Journal of Hydrologic Engineering*, 117:5(660), 660-667.

Titus, J. G. (1985). Potential impacts of sea level rise on the beach at Ocean City, Maryland. US Environmental Protection Agency, Office of Policy Planning and Evaluation.

Türker, U., & Kabdaşlı, M. S. (2006). The effects of sediment characteristics and wave height on shape-parameter for representing equilibrium beach profiles. *Ocean engineering*, 33(2), 281-291.

Wang, P., & Kraus, N. C. (2005). Beach profile equilibrium and patterns of wave decay and energy dissipation across the surf zone elucidated in a large-scale laboratory experiment. *Journal of Coastal Research*, 522-534.

Work, P. A., & Dean, R. G. (1991). Effect of varying sediment size on equilibrium beach profiles. *Coastal Sediments (ASCE)*, 890-904.

Wu, W., & Wang, S. (2006). Formulas for Sediment Porosity and Settling Velocity. *Journal of Hydraulic Engineering (ASCE)*, 132 (8), 858-862.

Özkan-Haller, H.T., & Brundidge, S. (2007). Equilibrium beach profile concept for Delaware Beaches. *Journal of Waterway, Port, Coastal, and Ocean Engineering*, 133 (2), 147–160.

APPENDICES

Appendix A: Settling velocity results conducted in hydraulic laboratory of Eastern Mediterranean University

Nominal diameter, d_n (m)	Shape factor, S_f	Specific gravity, S	Kinematic viscosity, ν (m^2s^{-1})	Settling velocity, ω (ms^{-1})	Particle Reynolds number, $Re_p = \frac{\omega \times d_n}{\nu}$
5.20×10^{-4}	1.00	4.45	8.27×10^{-7}	0.13274	83
5.80×10^{-4}	1.00	4.00	8.27×10^{-7}	0.13756	96
6.35×10^{-4}	1.00	4.00	8.27×10^{-7}	0.14545	112
6.30×10^{-4}	1.00	4.60	8.27×10^{-7}	0.16194	123
7.20×10^{-4}	1.00	4.45	8.27×10^{-7}	0.18924	165
7.50×10^{-4}	1.00	4.60	8.27×10^{-7}	0.19313	175
1.76×10^{-3}	0.77	4.43	1.16×10^{-6}	0.25901	392
2.28×10^{-3}	0.59	2.30	8.47×10^{-7}	0.15153	408
3.21×10^{-3}	0.44	2.10	8.46×10^{-7}	0.14054	534
2.33×10^{-3}	0.28	4.43	8.47×10^{-7}	0.20625	567
3.67×10^{-3}	0.32	2.30	8.47×10^{-7}	0.16685	723
4.90×10^{-3}	0.73	1.56	1.18×10^{-6}	0.17892	745
4.47×10^{-3}	0.86	1.70	1.18×10^{-6}	0.22500	854
4.40×10^{-3}	0.46	2.90	1.16×10^{-6}	0.23083	873
3.97×10^{-3}	0.61	2.10	8.46×10^{-7}	0.19120	898
3.15×10^{-3}	0.59	2.90	8.46×10^{-7}	0.24478	912
3.65×10^{-3}	0.37	3.30	8.47×10^{-7}	0.21418	923
5.78×10^{-3}	0.57	1.70	1.18×10^{-6}	0.19539	960
5.05×10^{-3}	0.50	2.34	1.18×10^{-6}	0.22730	975
5.40×10^{-3}	0.56	2.10	1.18×10^{-6}	0.23203	1065
4.00×10^{-3}	0.54	2.50	8.47×10^{-7}	0.23952	1131
5.05×10^{-3}	0.89	1.70	1.16×10^{-6}	0.26361	1145
4.91×10^{-3}	0.87	1.70	1.18×10^{-6}	0.28019	1169
5.45×10^{-3}	0.68	2.10	1.18×10^{-6}	0.25457	1179
5.48×10^{-3}	0.45	2.10	8.46×10^{-7}	0.19626	1272
5.85×10^{-3}	0.70	2.10	1.18×10^{-6}	0.26206	1302
5.05×10^{-3}	0.76	2.25	1.18×10^{-6}	0.31373	1346
5.73×10^{-3}	0.72	2.25	1.18×10^{-6}	0.29309	1427
4.23×10^{-3}	0.45	3.30	8.47×10^{-7}	0.28929	1445
4.49×10^{-3}	0.39	3.30	8.47×10^{-7}	0.27331	1449
6.44×10^{-3}	0.75	1.70	1.16×10^{-6}	0.26518	1467
5.48×10^{-3}	0.59	2.00	8.47×10^{-7}	0.23083	1493
4.97×10^{-3}	0.81	1.70	8.47×10^{-7}	0.25457	1494
5.51×10^{-3}	0.56	2.00	8.46×10^{-7}	0.23083	1504
5.58×10^{-3}	0.77	1.75	8.47×10^{-7}	0.23447	1545
6.00×10^{-3}	0.93	1.70	1.18×10^{-6}	0.30938	1577
5.13×10^{-3}	0.53	2.50	8.47×10^{-7}	0.26053	1578

Continued.

Nominal diameter, d_n (m)	Shape factor, S_f	Specific gravity, S	Kinematic viscosity, ν (m^2s^{-1})	Settling velocity, ω (ms^{-1})	Particle Reynolds number, $Re_p = \frac{\omega \times d_n}{\nu}$
5.38×10^{-3}	0.55	2.25	8.47×10^{-7}	0.25169	1599
5.06×10^{-3}	0.64	2.50	8.46×10^{-7}	0.27844	1666
6.46×10^{-3}	0.70	2.40	1.16×10^{-6}	0.31596	1755
6.95×10^{-3}	0.74	2.10	1.16×10^{-6}	0.29899	1786
5.64×10^{-3}	0.88	1.75	8.47×10^{-7}	0.26837	1787
5.35×10^{-3}	0.64	2.60	8.46×10^{-7}	0.28742	1819
6.23×10^{-3}	0.89	1.70	8.47×10^{-7}	0.26837	1974
6.02×10^{-3}	0.87	1.70	8.46×10^{-7}	0.28929	2060
5.58×10^{-3}	0.80	2.50	8.47×10^{-7}	0.33750	2224

Appendix B: Beach profiles

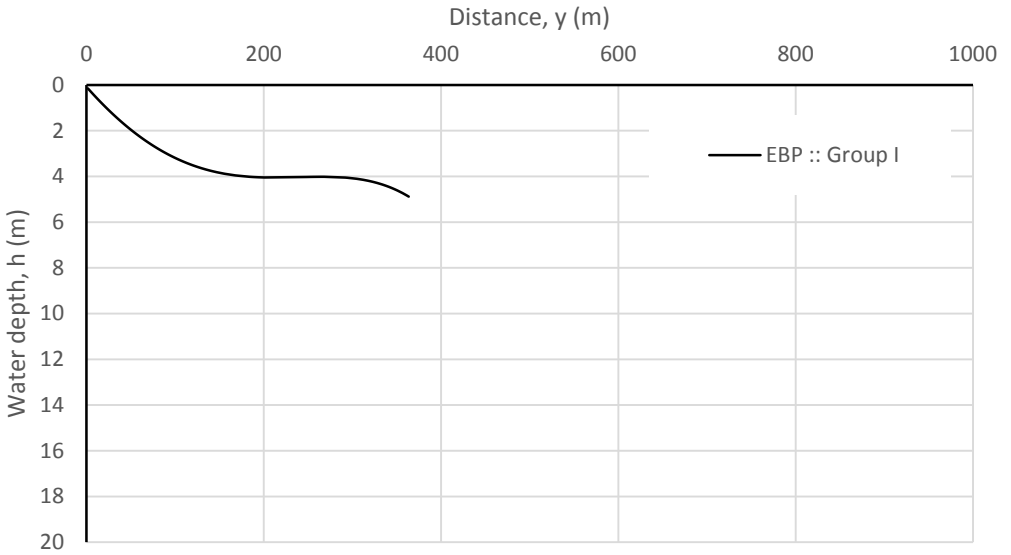

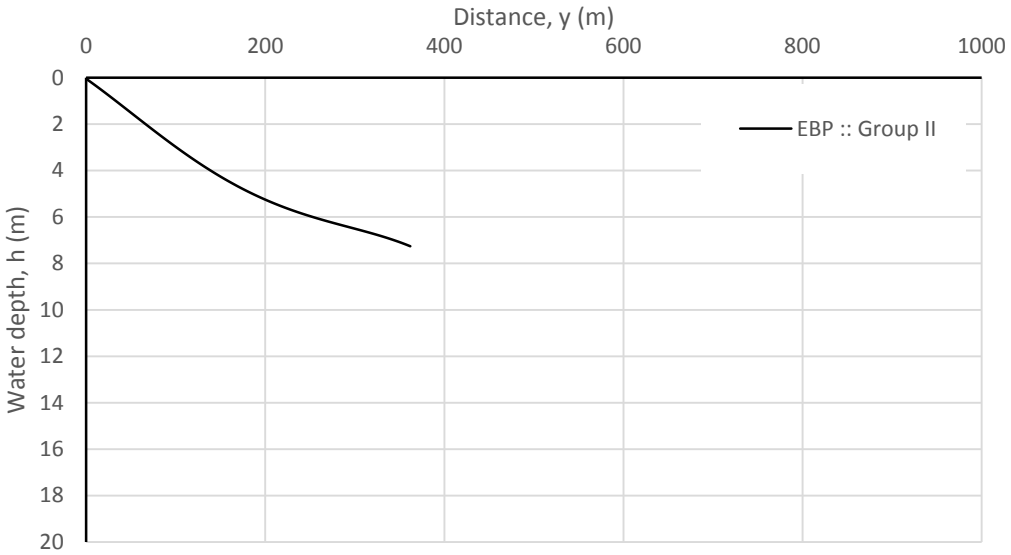

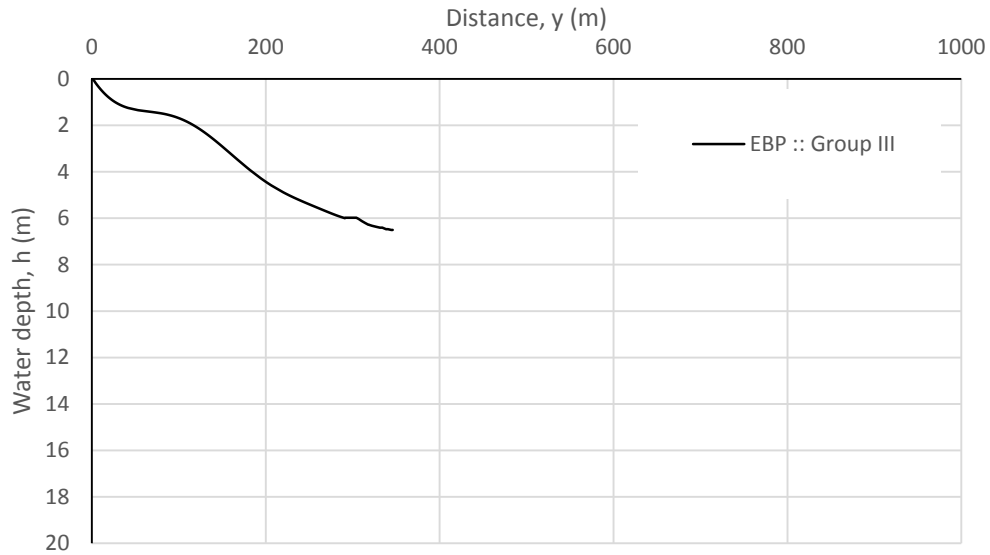

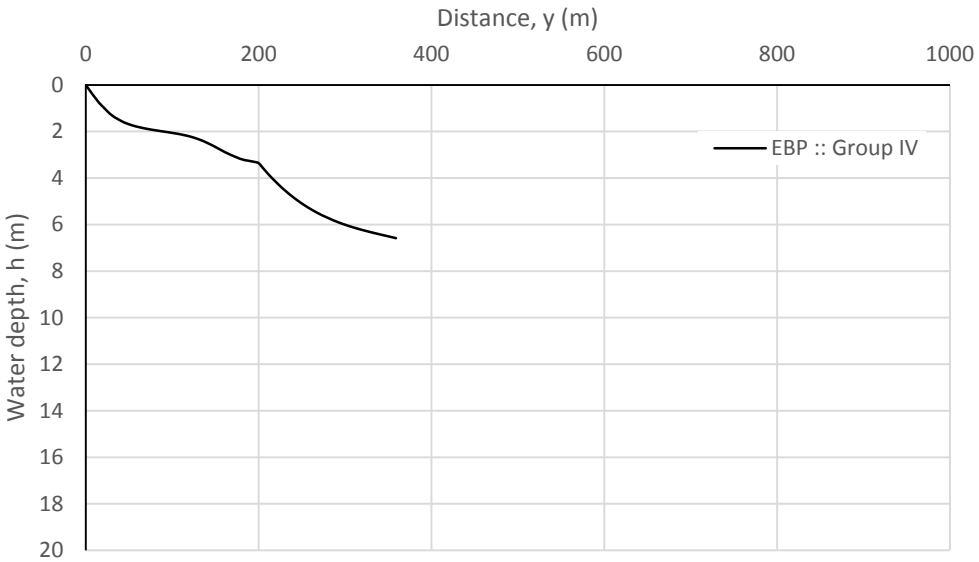
Distance, y (m)
0
200
400
600
800
1000
Water depth, h (m)
0
2
4
6
8
10
12
14
16
18
20
EBP :: Group IV

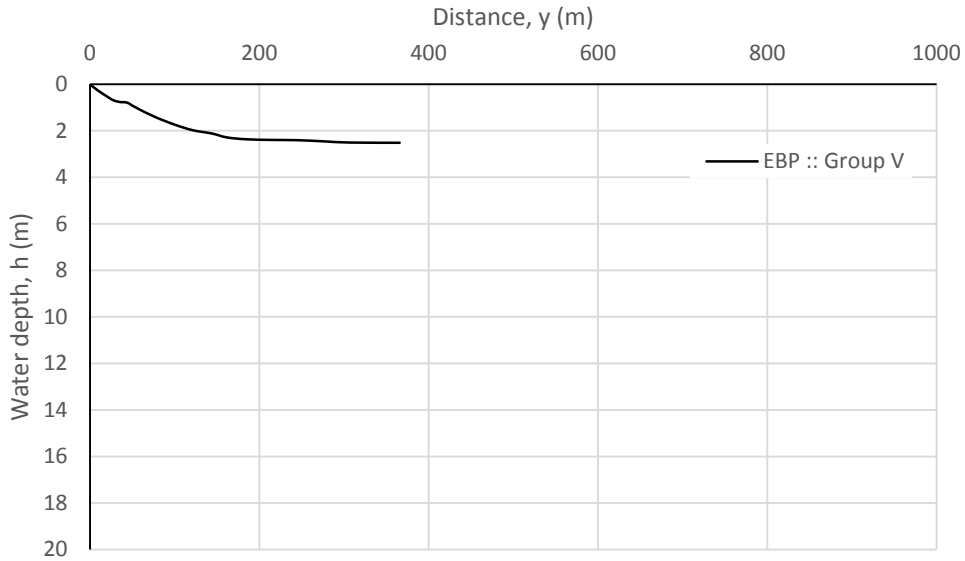
Distance, y (m)
0
200
400
600
800
1000
Water depth, h (m)
0
2
4
6
8
10
12
14
16
18
20
EBP :: Group V

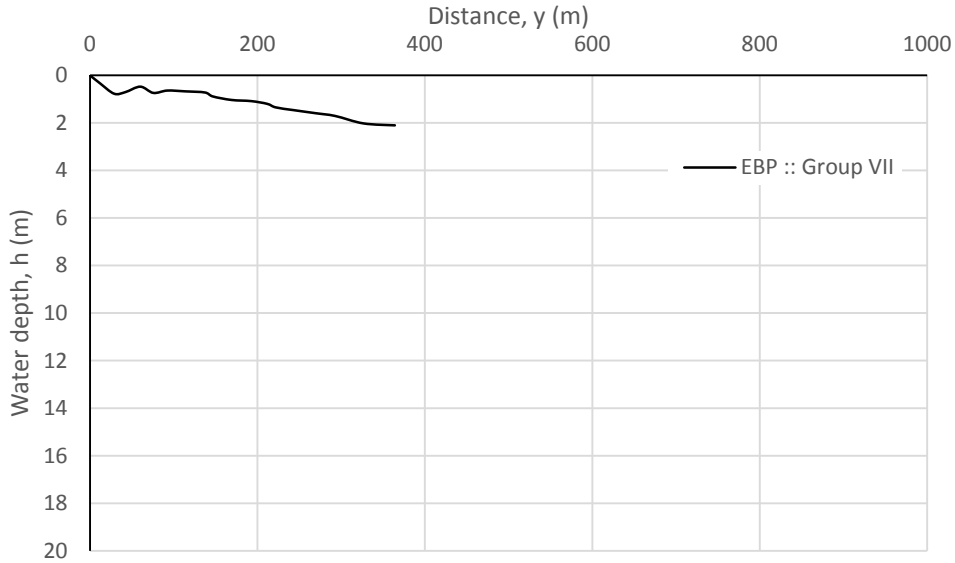
Distance, y (m)
0
200
400
600
800
1000
Water depth, h (m)
0
2
4
6
8
10
12
14
16
18
20
EBP :: Group VII

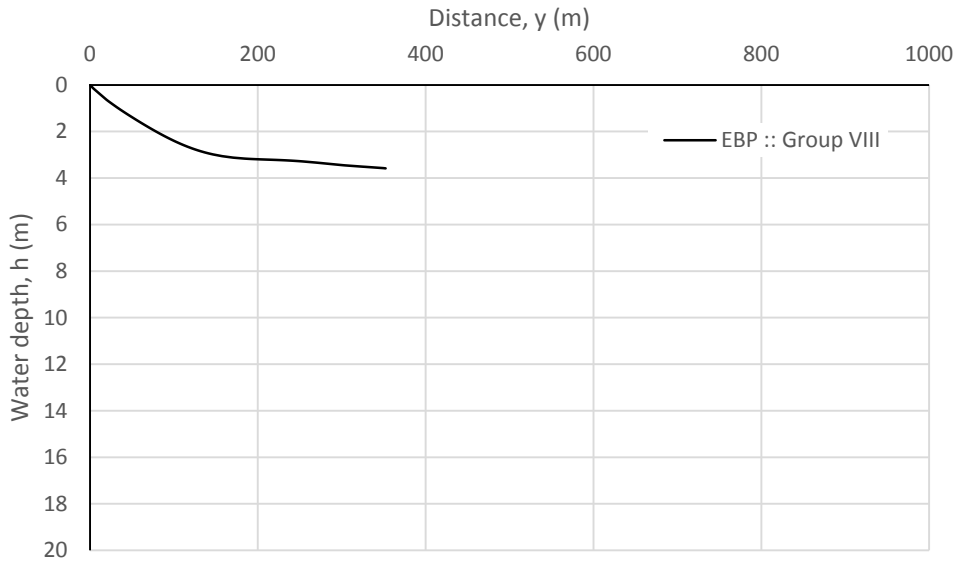
Distance, y (m)
0
200
400
600
800
1000
Water depth, h (m)
0
2
4
6
8
10
12
14
16
18
20
EBP :: Group VIII

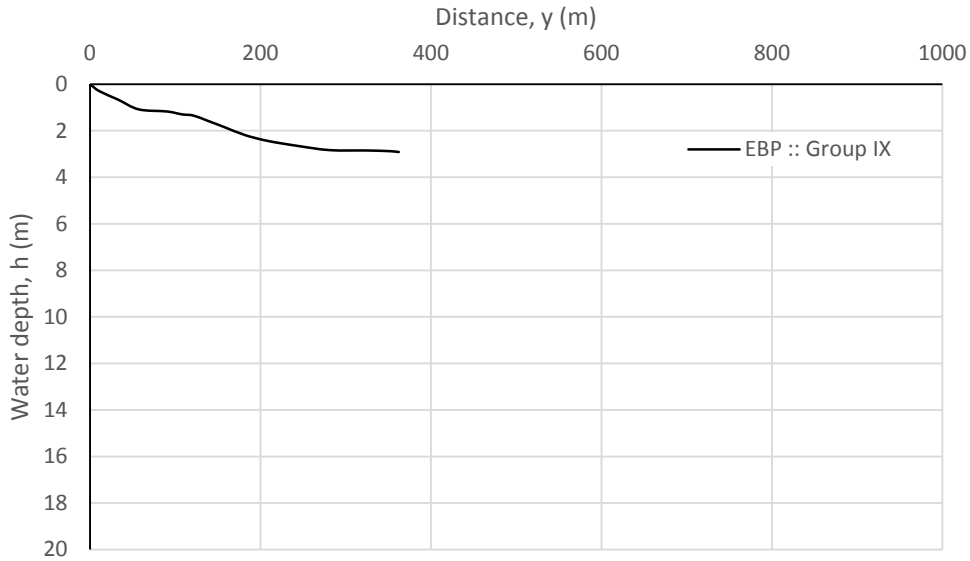
Distance, y (m)
0
200
400
600
800
1000
Water depth, h (m)
0
2
4
6
8
10
12
14
16
18
20
EBP :: Group IX

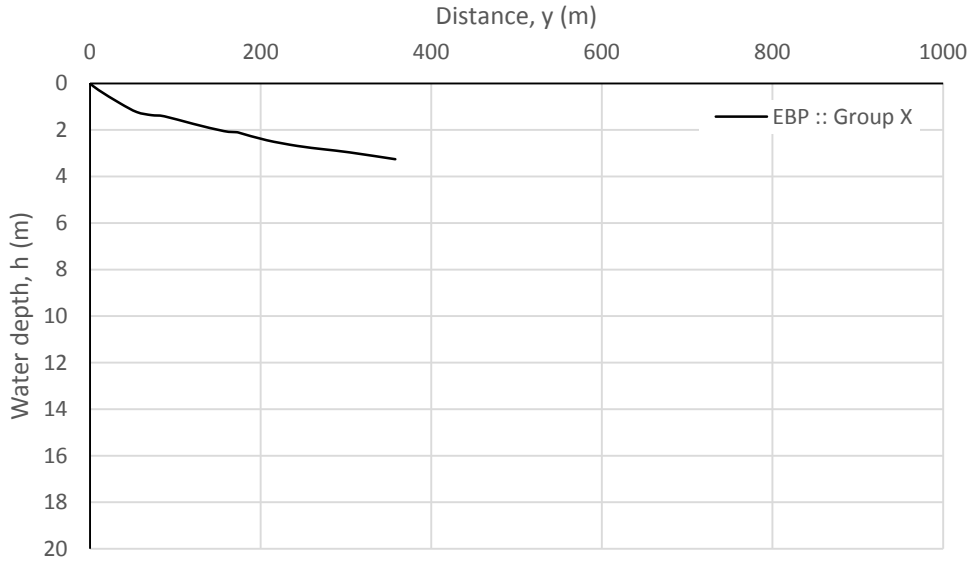
Distance, y (m)
0
200
400
600
800
1000
Water depth, h (m)
0
2
4
6
8
10
12
14
16
18
20
EBP :: Group X

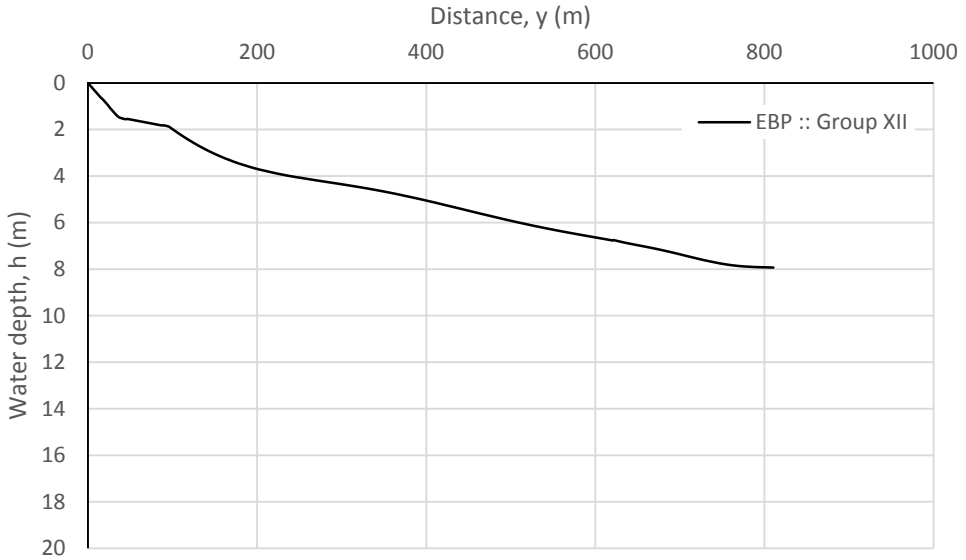
Distance, y (m)
0
200
400
600
800
1000
Water depth, h (m)
0
2
4
6
8
10
12
14
16
18
20
EBP :: Group XII

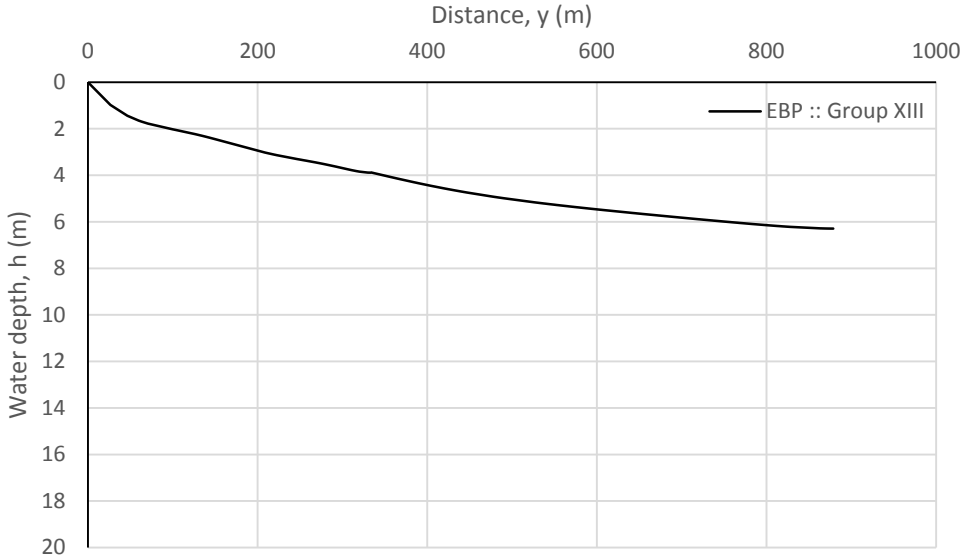
Distance, y (m)
0
200
400
600
800
1000
Water depth, h (m)
0
2
4
6
8
10
12
14
16
18
20
EBP :: Group XIII

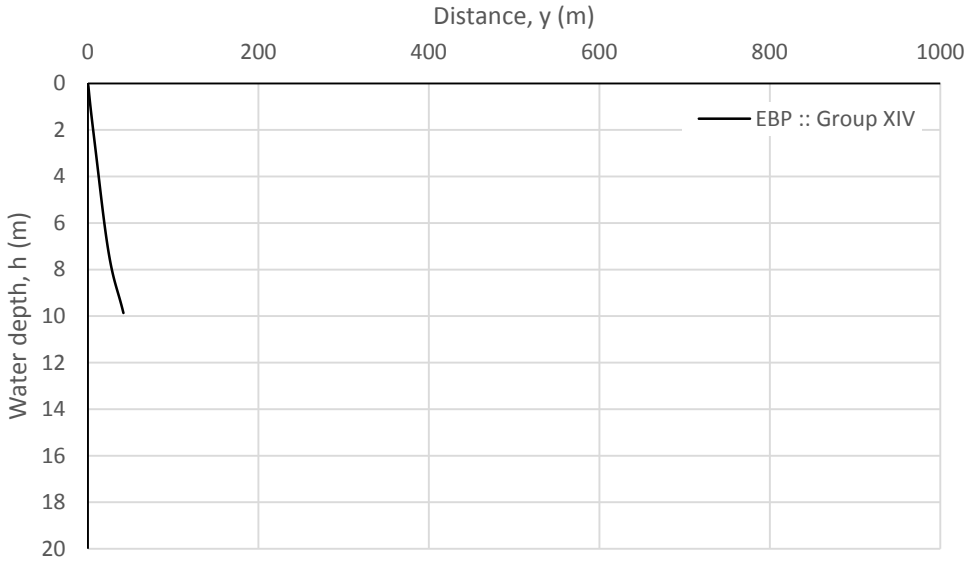
Distance, y (m)
0
200
400
600
800
1000
Water depth, h (m)
0
2
4
6
8
10
12
14
16
18
20
EBP :: Group XIV

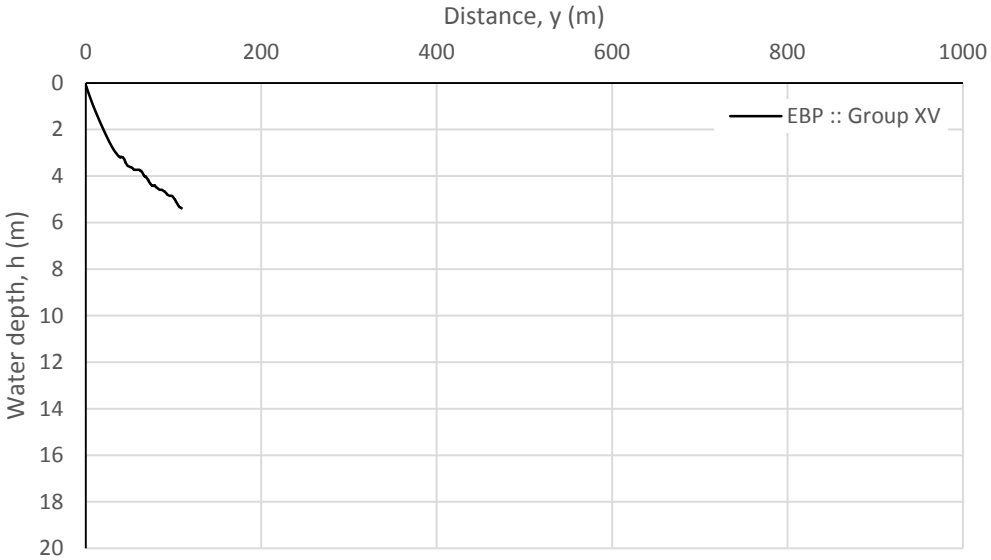
Distance, y (m)
0
200
400
600
800
1000
Water depth, h (m)
0
2
4
6
8
10
12
14
16
18
20
EBP :: Group XV

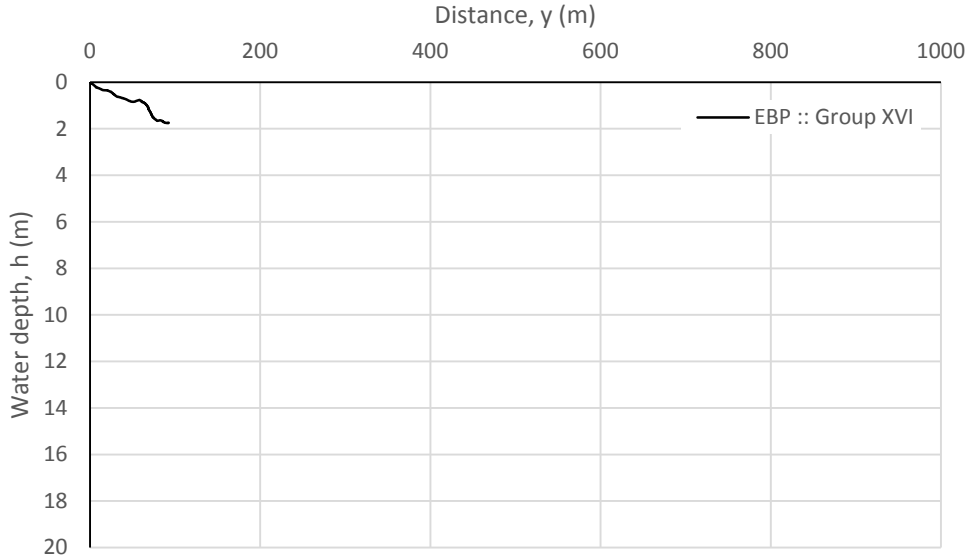
Distance, y (m)
0
200
400
600
800
1000
Water depth, h (m)
0
2
4
6
8
10
12
14
16
18
20
EBP :: Group XVI

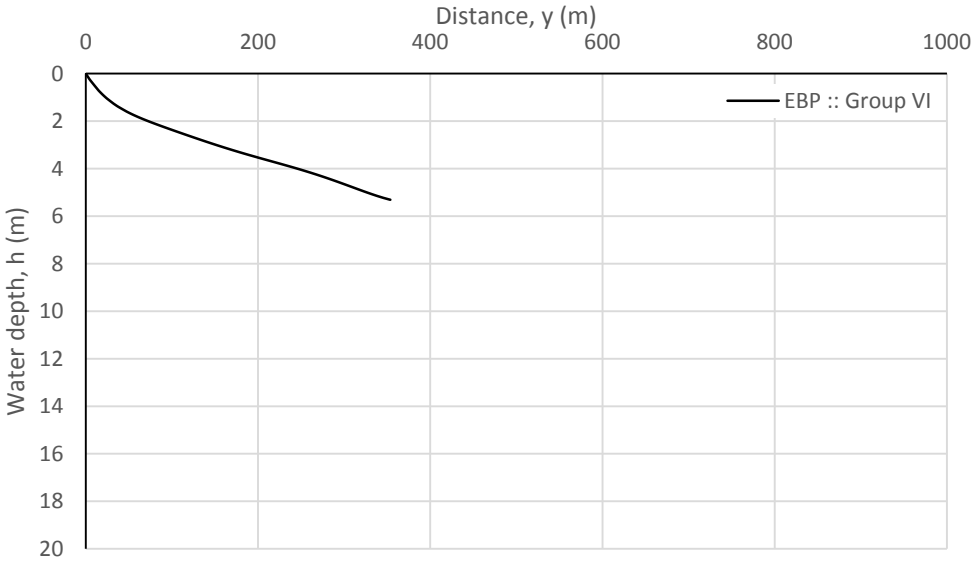
Distance, y (m)
0
200
400
600
800
1000
Water depth, h (m)
0
2
4
6
8
10
12
14
16
18
20
EBP :: Group VI

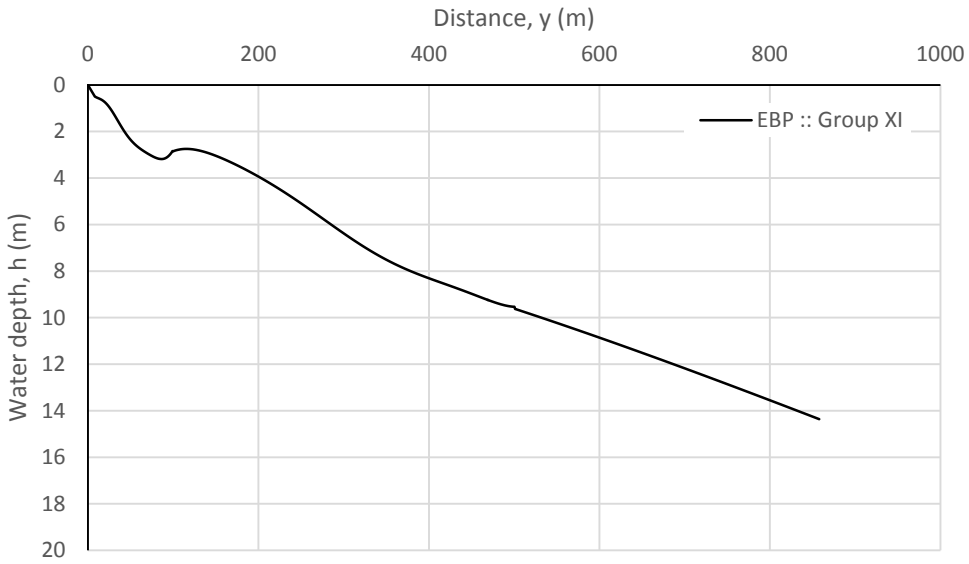
Distance, y (m)
0
200
400
600
800
1000
Water depth, h (m)
0
2
4
6
8
10
12
14
16
18
20
EBP :: Group XI